Chapter 3

Microwave Absorption and EMI Shielding Behavior of Nanocomposites Based on Intrinsically Conducting Polymers, Graphene and Carbon Nanotubes

Parveen Saini and Manju Arora

Additional information is available at the end of the chapter

http://dx.doi.org/10.5772/48779

1. Introduction

Electromagnetic interference (EMI) is an undesirable and uncontrolled off-shoot of explosive growth of electronics and widespread use of transient power sources. Conducting polymers nanocomposites represent a novel class of materials that possess unique combination of electrical, thermal, dielectric, magnetic and/or mechanical properties which are useful for suppression of electromagnetic noises. Now it is possible to incorporate various dielectric or magnetic fillers within conducting polymer matrices to form multifunctional nanocomposites. The first section of this chapter gives a brief overview of fundamentals of EMI shielding & microwave absorption, theoretical aspects of shielding, governing equations, various techniques for measurement of shielding effectiveness and different strategies for controlling EMI. In the next section, a comprehensive account of potential materials for handling of EMI are described with special reference to nanocomposites based on intrinsically conducting polymer matrix filled with conducting [e.g. metals, graphite, carbon back, carbon nanotubes, graphene], dielectric (e.g. $BaTiO_3$ or TiO_2) or magnetic (e.g. γ-Fe_2O_3, Fe_3O_4, $BaFe_{12}O_{19}$) inclusions.

2. Electromagnetic Interference (EMI) shielding

Electromagnetic interference shielding (EMI) is an undesired electromagnetic (EM) induction triggered by extensive use of alternating current/Voltage which tries to produce corresponding induced signals (Voltage and current) in the nearby electronic circuitry, thereby trying to spoil its performance. The mutual interference among electronic gadgets, business machines, process equipments, measuring instruments and appliances lead to disturbance or complete breakdown of normal performance of appliances. The EM

disturbances across communication channels, automation, and process control may lead to loss of time, energy, resources and also adversely affect human health. Due to these reasons only, use of mobile phone is restricted inside robotic operation theatres or during onboard/flight which may trigger series of electronic failures and a crash in worst case/scenario. Therefore, some shielding mechanism must be provided to ensure undisturbed functioning of devices even in the presence of external electromagnetic (EM) noises. For efficient shielding action, shield should possess either mobile charge carriers (electrons or holes) or electric and/or magnetic dipoles which interact with the electric (E) and magnetic (H) vectors of the incident EM radiation. Therefore, in the recent past, a wide variety of materials (Abbas et al, 2007; Colaneri et al, 1992; Joo & Epstein, 1994; Ott, 2009; Paul, 2004; Saini et al, 2009a, 2010, 2011; Schulz et al, 1988; Singh et al, 1999a, 2000b) have been used for EMI shielding with a broad range of electrical conductivity (σ), good electromagnetic attributes such as permittivity (ε) or permeability (μ) and engineered geometries. The designing a EMI shielding with a certain level of attenuation, meeting a set of physical criteria, maintaining economics and regulating the involved shielding mechanism is not a straight forward task and involves complex interplay of intrinsic properties (σ, ε and μ) of shield material and logical selection of extrinsic parameters. Therefore, to touch the theoretically predicted shielding performance of a materials and to satisfy stringent design criteria, elementary knowledge of shielding theory, set of governing theoretical equations, important design parameters and relevant measurement technique becomes a prime prerequisite.

3. Shielding definitions and phenomenon

EMI shield is essentially a barrier to regulate the transmission of the electromagnetic EM wave across its bulk. In power electronics, term shield usually refers to an enclosure that completely encloses an electronic product or a portion of that product and prevents the EM emission from an outside source to deteriorate its electronic performance.

Conversely, it may also be used to prevent an external susceptible (electronic items or living organisms) from internal emissions of an instrument's electronic circuitry. Shielding is the process by which a certain level of attenuation is extended using a strategically designed EM shield. The shielding efficiency is generally measured in terms of reduction in magnitude of incident power/field upon transition across the shield. Mathematically shielding effectiveness (SE_T) can be expressed in logarithmic scale as per expressions (Saini et al 2009a, 2011):

$$SE_T\,(dB) = SE_R + SE_A + SE_M = 10\log_{10}\left(\frac{P_T}{P_I}\right) = 20\log_{10}\left(\frac{E_T}{E_I}\right) = 20\log_{10}\left(\frac{H_T}{H_I}\right) \quad (1)$$

where P_I (E_I or H_I) and P_T (E_T or H_T) are the power (electric or magnetic field intensity) of incident and transmitted EM waves respectively. As shown in Fig. 1, three different mechanisms namely reflection (R), absorption (A) and multiple internal reflections (MIRs) contribute towards overall attenuation with SE_R, SE_A and SE_M as corresponding shielding effectiveness components due to reflection, absorption and multiple reflections respectively.

3.1. Theoretical shielding effectiveness

Before starting the shielding analysis, it is necessary to understand the various electromagnetic terminologies (Ott, 2009).

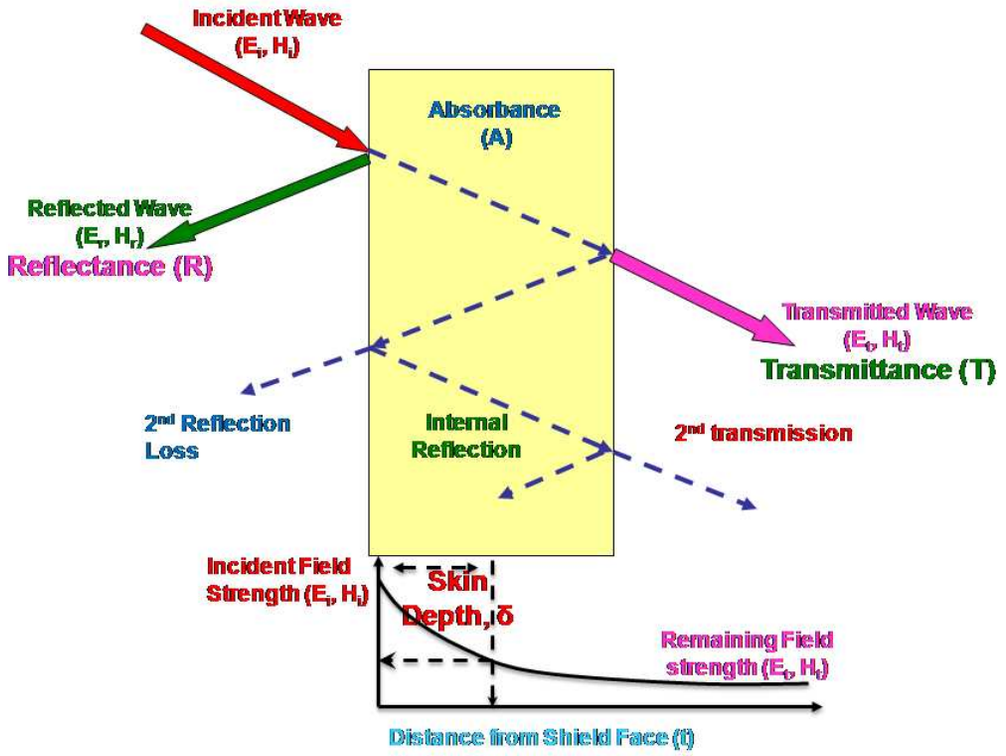

Figure 1. Schematic representation of EMI shielding mechanism

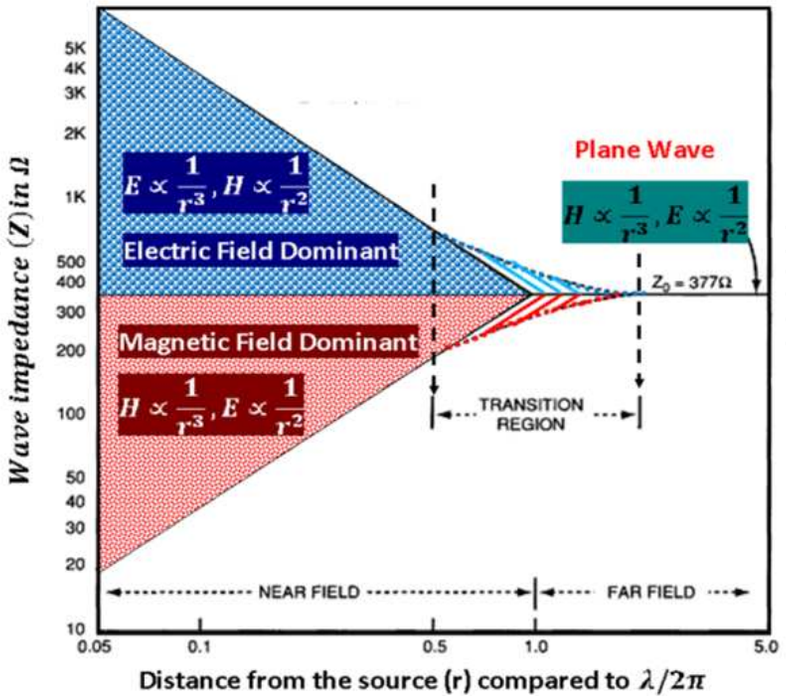

Figure 2. Dependence of wave impedance on distance from source normalized to λ/2π

According to the distance r between the radiating source and the observation point, an electromagnetic radiative region can be divided into three parts (Fig. 2) relative total wavelength λ of the electromagnetic wave. The region within the distance $r < \lambda/2\pi$ is the near field while the distance $r > \lambda/2\pi$ is the far field. Between the two regions, as the distance $r \approx \lambda/2\pi$, is the transition region. For designing a material for particular shielding application, it is imperative to have in-depth knowledge of both intrinsic & extrinsic parameters on which shielding effectiveness depend alongwith suitable theoretical relations correlating them with reflection, absorption and multiple-reflection loss components.

3.1.1. Shielding theory

This section presents the shielding basics based on the transmission line theory (Schelkunoff, 1943) and the plane wave shielding theory (Schulz et al,1988). Assume a uniform plane wave characteristic by E and H that vary within a plane only with x direction as showed in Fig. 3. The Maxwell's curl equations give:

$$\frac{dE}{dx} = -j\omega\mu H \text{ and } \frac{dH}{dx} = -(\sigma + j\omega\varepsilon)E \tag{2}$$

where μ is the permeability of the material and $\mu = \mu_o\mu_r$. μ_o and μ_r are the permeabilities of air (*or free space*) and shield material respectively, σ is the conductivity of material in *S/m*. where ε is the permittivity of the material and $\varepsilon = \varepsilon_o\varepsilon_r$. ε_o and ε_r are the permittivities of air (or free space) and shield material respectively, $\omega = 2\pi f$. ω (f) is angular frequency (linear frequency) in Hz.

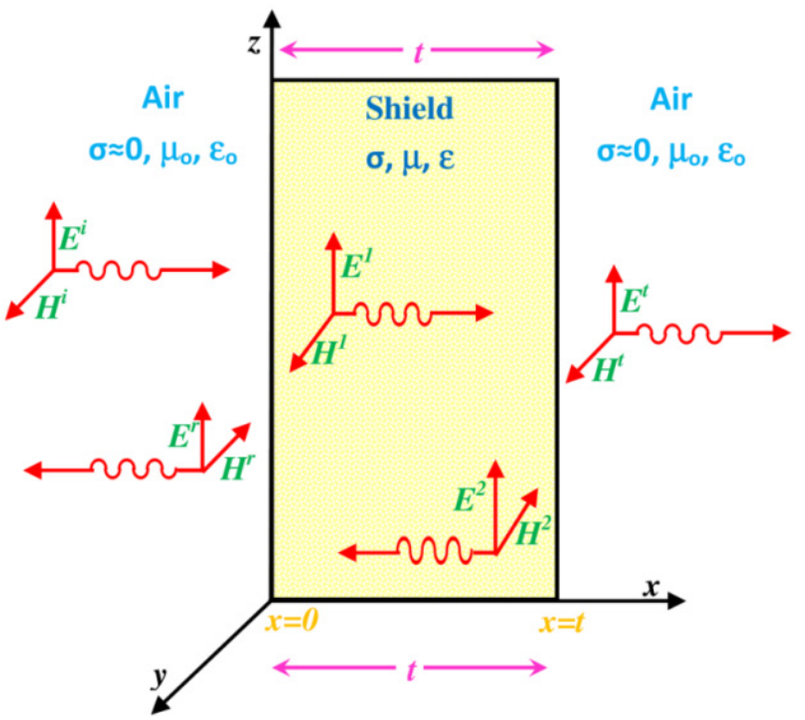

Figure 3. Propagation of electromagnetic waves and its interaction with the shield material

All homogenous materials are characterized by a quantity known as the intrinsic impedance:

$$\eta = \sqrt{\frac{j\omega\mu}{\sigma + j\omega\varepsilon}} \tag{3}$$

When an electromagnetic wave propagates through the material, the wave impedance approaches the intrinsic impedance of the material. For dielectric material, the conductivity is extremely small ($\sigma \ll \omega\varepsilon$) and the intrinsic impedance of Eq. (3) becomes:

$$\eta = \sqrt{\frac{\mu}{\varepsilon}} \tag{4}$$

For a conductor used below optical frequencies defined by $\sigma \gg \omega\varepsilon$, the intrinsic impedance of Eq. (3) can be written as:

$$\eta = \sqrt{\frac{j\omega\mu}{\sigma}} = (1+j)\sqrt{\frac{\pi\mu f}{\sigma}} \tag{5}$$

It is customary to define propagation constant (γ) in the media such that:

$$\gamma = (\alpha + j\beta) = \sqrt{j\omega\mu(\sigma + j\omega\varepsilon)}. \tag{6}$$

where α is attenuation constant and β is phase constant. A good conductor is a medium for which $\sigma / \omega\varepsilon \gg 1$. Under this condition the Eq. (6) becomes:

$$\gamma = \sqrt{j\omega\mu} = (1+j)\sqrt{\pi\mu f\sigma} \tag{7}$$

Therefore, we can write $\alpha = \beta = 1/\delta = \sqrt{\pi\mu f\sigma}$, where quantity δ represents skin depth which is defined as the distance required by the wave to be attenuated to $1/e$ or 37% of its original strength. For a dielectric plane sheet $\sigma / \omega\varepsilon \ll 1$ and Eq. (6) becomes:

$$\gamma = \sqrt{-\omega^2\mu\varepsilon} = j\omega\sqrt{\mu\varepsilon} \tag{8}$$

The impedance of a homogenous barrier of thickness t is

$$Z = \eta\frac{Z(t)\cosh(\gamma t) + \eta\sinh(\gamma t)}{\eta\cosh(\gamma t) + Z(t)\sinh(\gamma t)} \tag{9}$$

$$H(t) = \frac{\eta}{\eta\cosh(\gamma t) + Z(t)\sinh(\gamma t)}H(0) \tag{10}$$

$$E(t) = \frac{Z(t)}{Z(t)\cosh(\gamma t) + \eta\sinh(\gamma t)}E(0) \tag{11}$$

where $Z(0)$ is the impedance at interface 0 looking into the plane and $H(t)$ is the impedance at interface t looking into the right of the plane at $x = t$. If $Z(t) \neq \eta$, reflection

occurs at the boundary $x = t$. Let E^i and H^i are the incident electric and magnetic fields, E^r and H^r the reflected fields, and E^t and H^t the transmitted fields as shown in Fig. 3. With the continuity of the tangential field component at a boundary we can write:

$$E^i + E^r = E^t \quad \text{and} \quad H^i + H^r = H^t \tag{12}$$

The electric and magnetic fields of a plane wave are related by the intrinsic impedance of the medium

$$E^i = \eta H^i, \; E^r = -\eta H^r \text{ and } E^t = Z(l)H^i \tag{13}$$

Solving the above equations, the expression of reflection coefficients can be written as:

$$q_E = \frac{E^r}{E^i} = \frac{Z(t) - \eta}{Z(t) + \eta} \tag{14}$$

$$q_H = \frac{H^r}{H^i} = \frac{\eta - Z(t)}{\eta + Z(t)} = -q_E \tag{15}$$

The corresponding transmission coefficients can be written as:

$$p_E = \frac{E^t}{E^i} = \frac{2Z(t)}{\eta + Z(t)} = 1 + q_E \tag{16}$$

$$p_H = \frac{H^t}{H^i} = \frac{2\eta}{\eta + Z(t)} = 1 + q_H \tag{17}$$

When two mismatched interfaces must be considered in the same plane, the net transmission coefficients is the product of the transmission coefficient across the two boundaries i.e.:

$$p = p_E = p_H = p_E(0)p_E(t) = p_H(0)p_H(t) \tag{18}$$

Considering the re-reflection effect, the transmission coefficients across the plane are:

$$T_H = \frac{H(t)}{H^i} = \frac{H(t)}{H(0)} . \frac{H(0)}{H^i} \tag{19}$$

$$T_E = \frac{E(t)}{E^i} = \frac{Z(t)}{Z_w} . \frac{H(t)}{H^i} = \frac{Z(t)}{Z_w} T_H \tag{20}$$

where $E(0)$, $E(t)$, $H(0)$ and $H(t)$ are the actual values at interfaces i.e. at $x = 0$ and $x = t$. Z_w is the impedance of the incident wave. Using equations (9), (10) and (11) for the plane of the thickness 0 and t

$$\frac{H(t)}{H(0)} = \frac{\eta}{\eta \cosh(\gamma t) + Z(t) \sinh(\gamma t)} \tag{21}$$

$$\frac{E(t)}{E(0)} = \frac{Z(t)}{Z(t)\cosh(\gamma t) + \eta \sinh(\gamma t)} \tag{22}$$

From equations (14) and (15) we may write:

$$\frac{H(t)}{H^i} = \frac{2Z_w}{Z_w + Z(0)} \tag{23}$$

$$\frac{E(t)}{E^i} = \frac{2Z(0)}{Z_w + Z(0)} \tag{24}$$

where $Z(0)$ is the impedance at interface $x = 0$ looking into the plane. By substituting (23) and (24) into equations (19) and (20) we get:

$$T = T_E = p_H\left(1 - q_H e^{-2\gamma t}\right)e^{-\gamma t} \tag{25}$$

where

$$p_H = \frac{4Z_w\eta}{\left(Z_w + \eta\right)\left(Z(t) + \eta\right)} \tag{26}$$

$$q_H = \frac{\left(Z_w - \eta\right)\left(Z(t) - \eta\right)}{\left(Z_w + \eta\right)\left(Z(t) + \eta\right)} \tag{27}$$

when $Z(t) = Z_w$, taking $k = Z_w / \eta$ we can write:

$$p = p_H = \frac{4k}{\left(k+1\right)^2} \tag{28}$$

$$q = q_H = \frac{\left(k-1\right)^2}{\left(k+1\right)^2} \tag{29}$$

$$T_E = T_H \;=\; T = p\left(1 - qe^{-2\gamma t}\right)e^{-\gamma t} \tag{30}$$

By definition total shielding effectiveness is:

$$SE_T = 20\log_{10}|T| = 20\log_{10}\left|p\left(1 - qe^{-2\gamma t}\right)e^{-\gamma t}\right| \tag{31}$$

$$SE_T = \underbrace{20\log_{10}|p|}_{SE_R} + \underbrace{20\log_{10}\left|e^{-\gamma t}\right|}_{SE_A} + \underbrace{20\log_{10}\left|\left(1 - qe^{-2\gamma t}\right)\right|}_{SE_M} \tag{32}$$

Therefore, after careful comparison of δ with shield thickness (t) two situations can be visualized:

a. **When (t << δ):** which occurs either at low frequencies or in case of electrically thin sample where actual shield thickness is much less than skin depth. In such a case the absorption which is a bulk (or thickness) related phenomenon, can be neglected and attenuation occurs almost exclusively by reflection. The total shielding becomes frequency independent and can be expressed in terms of free space impedance (Z_o=377 Ω) as:

$$\mathrm{SE\,(dB)} = -20\log_{10}\left[1+\frac{Z_O}{2}t\sigma_T\right] \tag{33}$$

b. **When (t >> δ):** which is valid in our case and generally occurs at higher frequencies where skin depth becomes much less as compared to actual shield thickness i.e. in case of electrically thick samples. In such regime, attenuations due reflection, absorption and multiple internal sub-phenomenon becomes a straight forward exercise after making good conductor approximation i.e. $\sigma_T / \omega\varepsilon \gg 1$ [or $k \ll 1\left(i.e.\, Z_w \gg \eta\right)$].

3.1.2. Reflection loss

The reflection loss (SE_R) is related to the relative impedance mismatch between the shield's surface and propagating wave. The magnitude of reflection loss under plane wave (far field conditions) can be expressed as (Saini et al, 2011):

$$\mathrm{SE_R\,(dB)} = -10\log_{10}\left(\frac{\sigma_T}{16\omega\varepsilon_o\mu_r}\right) \tag{34}$$

where σ_T is the total conductivity, f is the frequency in Hz, μ_r is the relative permeability referred to free space; The above expression shows that SE_R is a function of the ratio of conductivity (σ_T) and permeability (μ_r) of the shield material i.e. quantity (σ_T/μ_r). Further, for a given material (i.e. fixed σ_T and μ_r) SE_R decreases with increase in frequency.

3.1.3. Absorption loss

As shown in Fig. 1, when an electromagnetic wave pass through a medium its amplitude decreases exponentially. This decay or absorption loss occurs because currents induced in the medium produce ohmic losses and heating of the material, and E_t and H_t can be expressed as $E_t = E_i e^{-t/\delta}$ and $H_t = H_i e^{-t/\delta}$ (Ott, 2009). Therefore, the magnitude of absorption term (SE_A) in decibel (dB) can be expressed by following equation:

$$\mathrm{SE_A\,(dB)} = -20\frac{t}{\delta}\log_{10} e = -8.68\left(\frac{t}{\delta}\right) = -8.68t\left(\frac{\sigma_T\omega\mu_r}{2}\right)^{\frac{1}{2}} \tag{35}$$

where t is shield thickness in inches and f is frequency in Hertz. The above expression revealed that SE_A is proportional to the square root of the product of the permeability (μ_r)

times the conductivity (σ_T) of the shield material i.e. quantity $(\sigma_T.\mu_r)^{1/2}$ (Saini et al, 2009a, 2011). Further, for a given material, absorption loss increases with increase in frequency. Therefore, a good absorbing material should possess high conductivity and high permeability, and sufficient thickness to achieve the required number of skin depths even at the lowest frequency of concern.

3.1.4. Multiple Internal Reflections (MIRs)

If the shield is thin, the reflected wave from the second boundary is re-reflected from the first boundary and returns to the second boundary to be reflected again and again as shown in Fig. 1. The attenuation due these multiple internal reflections i.e. SE_M can be mathematically expressed as (Ott, 2009, Saini et al, 2011):

$$SE_M = 20\log_{10}(1-e^{-2t/\delta}) = 20\log_{10}\left|\left(1-10^{-\frac{SE_A}{10}}\right)\right| \tag{36}$$

Therefore, it can be seen from the above expression that SE_M is closely related to absorption loss (SE_A). SE_M is also important for porous structures and for certain type of filled composites or for certain design geometries. It can be neglected in the case of a thick absorbing shield due high value of SE_A so that by the time the wave reaches the second boundary, it is of negligible amplitude. For practical purposes, when SE_A is ≥ 10 dB (Saini, et al 2009a, 2011) SE_M can be safely neglected. Usually SE_M is important only when metals are thin and are used at very low frequencies (i.e. ~kHz range). However, for highly absorbing materials or at very high frequencies (~GHz or high), condition $|SE_A| \geq 10dB$ gets satisfied and re-reflections can be safely ignored i.e. $SE_M \approx 0$.

3.2. Experimental shielding effectiveness

Experimentally, shielding is measured using instruments called network analyzer. Scalar network analyzer (SNA) measures only the amplitude of signals whereas vector network analyzer (VNA) measures magnitude as well as phases of various signals. Consequently, SNA can not be used to measure complex signals (e.g. complex permittivity or permeability) and therefore, despite its higher cost VNA is the most widely used instrument.

The incident and transmitted waves in a two port VNA (Fig. 4) can be mathematically represented by complex scattering parameters (or S-parameters) i.e. S_{11} (or S_{22}) and S_{12} (or S_{21}) respectively which in-turn can be conveniently correlated with reflectance (R) and transmittance (T) i.e. $T = |E_T/E_I|^2 = |S_{12}|^2 = |S_{21}|^2$, $R = |E_R/E_I|^2 = |S_{11}|^2 = |S_{22}|^2$, giving absorbance (A) as: A = (1-R-T). When SE_A is greater than 10 dB, SE_M becomes negligible (~ -1.0 dB) and can be neglected (Saini et al, 2011) so that SE_T can be expressed as: $SE_T = SE_R + SE_A$. In addition, the intensity of the EM wave inside the shield after primary reflection is based on quantity (1-R), which can be subsequently used for normalization of absorbance (A) to yield effective absorbance $\{A_{eff}=[(1-R-T)/(1-R)]\}$ so that experimental reflection and absorption losses can be expressed as (Hong et al, 2003; Saini et al, 2009a, 2011):

$$SE_R = 10\log_{10}(1 - R) \tag{37}$$

$$SE_A = 10\log_{10}(1 - A_{eff}) = 10\log_{10}\left[\frac{T}{(1 - R)}\right] \tag{38}$$

Therefore, from the knowledge of reflected and transmitted signals i.e. R and T, VNA can easily compute reflection and absorption loss components of total shielding.

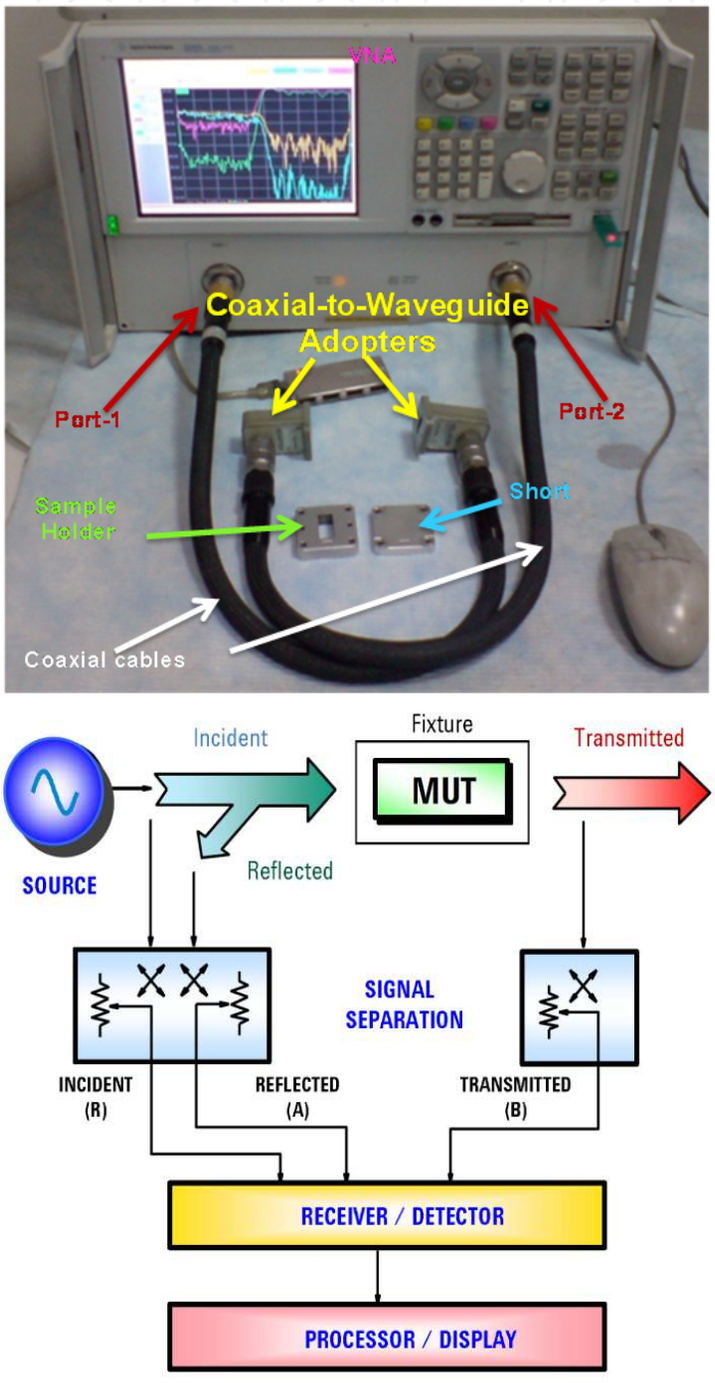

Figure 4. A two port VNA (left) and its internal block diagram (right)

3.3. Estimation of electromagnetic attributes

The attenuation of EM radiation by intended shield material is critically dependent on its electromagnetic attributes like complex permittivity [$\varepsilon^* = (\varepsilon' \; j\varepsilon'')$] and complex permeability [$\mu^* = (\mu' \; j\mu'')$], and their estimation is of paramount importance. Both complex dielectric permittivity and magnetic permeability consists of real part and imaginary parts as shown in Fig. 5

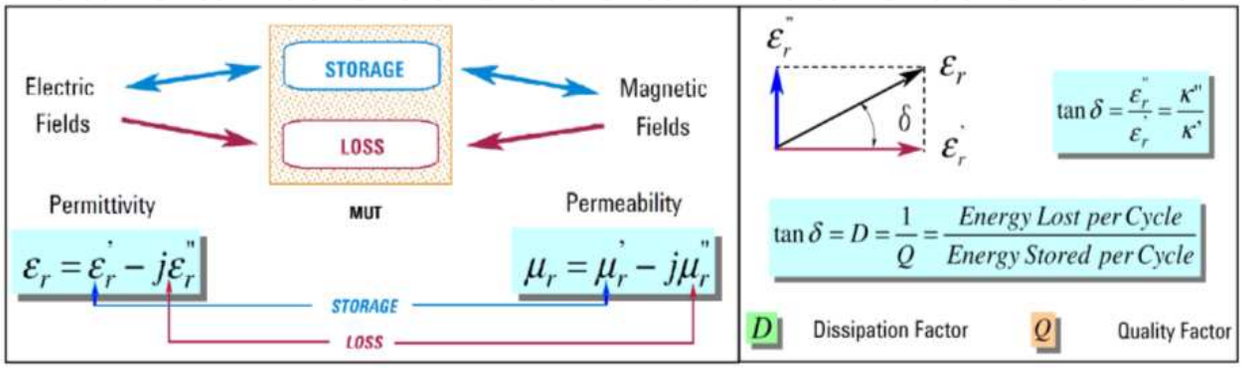

Figure 5. Complex electromagnetic attributes of a shield

Parameter ε' or ε_r (real permittivity) represents the charge storage (or dielectric constant) whereas ε'' (imaginary permittivity) is a measure of dielectric dissipation or losses. Similarly, μ' (or ε_r) and μ'' represents magnetic storage and losses respectively. The extent of losses can be assessed by calculating dielectric/magnetic loss tangent (tan δ) (Colaneri et al, 1992; Joo. et al, 1994; Saini. et al, 2009a, 2011) which is the ratio of imaginary and real permittivity/permeability.

3.3.1. Measurement and conversion techniques

While designing a shield, all the above parameters must be taken into consideration. The incident and transmitted travelling waves inside a VNA can be represented by complex scattering parameters (or S-parameters) i.e. S_{11} (or S_{22}) and S_{12} (or S_{21}) respectively, which are in-turn closely related to the electromagnetic (EM) attributes (Nicolson & Ross, 1970; Ott, 2009; Paul, 2004; Weir, 1974). There are many techniques developed for measuring these S-parameters like Transmission/Reflection method, Open ended coaxial probe technique, Free space technique, Resonant cavity method and Parallel plate technique (Ott, 2009; Tong, 2009). Among these techniques Transmission/Reflection method is the most popular as it simultaneously measures of all four S-parameters and gives complex permittivity as well as magnetic permeability by using suitable algorithms or models developed for obtaining the permittivity and permeability from the recorded S-parameters. Table 1 gives an overview of some the conversion techniques, S-parameters & to and their evaluation capability for output attributes.

Each of the above conversion technique has different advantages and limitations. The selection of the technique depends on several factors such as the measured S-parameters, sample length, desired output properties, speed of conversion and accuracies in the converted results. Among

above-mentioned procedures, Nicholson-Ross-Weir (NRW) technique is the most widely used regressive/iterative analysis as it provides direct calculation of both the permittivity (ε^*) and permeability (μ^*) from the input S-parameters.

Conversion technique	**Input S-parameters**	**Output attributes**
Nicolson-Ross-Weir (NRW)	S_{11}, S_{21}, S_{12} and S_{22} or and S_{11} and S_{21} (or S_{22} and S_{12})	ε_r and μ_r
NIST iterative	S_{11}, S_{21}, S_{12} and S_{22} or pair S_{11} and S_{21} (or S_{22} and S_{12})	ε_r and $\mu_r = 1$
New non-iterative	S_{11}, S_{21}, S_{12} and S_{22} or and S_{11} and S_{21} (or S_{22} and S_{12})	ε_r and $\mu_r = 1$
Short circuit line (SCL)	S_{11} or S_{22}	ε_r

Table 1. Conversion techniques, input S-parameters & output attributes

3.3.2. Nicholson-Ross-Weir (NRW) technique

Nicholson-Ross-Weir (NRW) technique (Nicolson & Ross, 1970; weir, 1974) provides direct calculation of both the permittivity (ε^*) and permeability (μ^*) from the input S-parameters. It is the most commonly used technique for performing such conversions where the measurement of reflection (Γ) and transmission (T) coefficient requires all four (S_{11}, S_{21}, S_{12}, S_{22}) or a pair (S_{11}, S_{21}) of S-parameters of the material under test to be measured. The procedure proposed by NRW method is deduced from the following set of equations:

$$S_{11} = \frac{\Gamma\left(1-T^2\right)}{\left(1-\Gamma^2T^2\right)} \quad \text{and} \quad S_{21} = \frac{T\left(1-\Gamma^2\right)}{\left(1-\Gamma^2T^2\right)} \tag{39}$$

Once these S-parameters are extracted from the network analyzer, simultaneous solving of equation set (39) gives the reflection coefficient as:

$$\Gamma = X \pm \sqrt{X^2-1} \tag{40}$$

The condition [$|\Gamma| < 1$] is used for finding the correct root of the quadratic equation so that parameter X can be expressed as:

$$X = \frac{S_{11}^2 - S_{21}^2 + 1}{2S_{11}} \tag{41}$$

Therefore, the transmission coefficient can be written as:

$$T = \frac{S_{11} + S_{21} - \Gamma}{1-\left(S_{11}-S_{21}\right)\Gamma} \tag{42}$$

The permeability is then given by:

$$\mu^* = \frac{1+\Gamma}{\Lambda(1-\Gamma)\sqrt{\frac{1}{\lambda_o^2}-\frac{1}{\lambda_c^2}}} \tag{43}$$

where λ_o and λ_c are free space and cutoff wavelength respectively and Λ is given by (Tong, 2009):

$$\frac{1}{\Lambda^2} = \left(\frac{\varepsilon^* \mu^*}{\lambda_o^2} - \frac{1}{\lambda_c^2}\right) = -\left[\frac{1}{2\pi L}\ln\left(\frac{1}{T}\right)\right]^2 \tag{44}$$

Therefore, the permittivity can be written as:

$$\varepsilon^* = \frac{\lambda_o^2}{\mu^*}\left(\frac{1}{\lambda_c^2} - \left[\frac{1}{2\pi L}\ln\left(\frac{1}{T}\right)\right]^2\right) \tag{45}$$

Equations (44) & (45) have infinite number of roots since the imaginary part of the term ln(1/T) is equal to i(θ + 2πn) where n= 0, ± 1, ± 2…, i.e. the integral multiples of ratio L/λ_g, where L is sample length and λ_g is wavelength inside the sample. This brings phase ambiguity and the correct value of 'n' can be determined by either of two methods:

a. The analysis of group delay:

The calculated group delay for n^{th} solution can be determined from:

$$\tau_{cal,n} = L\frac{d}{df}\left(\sqrt{\frac{\varepsilon_r \mu_r f^2}{c^2} - \frac{1}{\lambda_c^2}}\right) = \frac{\left(f\varepsilon_r\mu_r + \frac{f^2}{2}\frac{d(\varepsilon_r\mu_r)}{df}\right)}{c^2\sqrt{\frac{\varepsilon_r\mu_r f^2}{c^2} - \frac{1}{\lambda_c^2}}}L \tag{46}$$

The group can also be directly measured by network analyzer by measuring the slope of the plot between phase (ϕ) of the transmission coefficient versus frequency as:

$$\tau_{meas} = -\frac{1}{2\pi}\frac{d\phi}{df} \tag{47}$$

The correct root (n=k) should satisfy the condition $\tau_{cal,k} - \tau_{meas} = 0$

b. Phase unwrapping method:

By estimating n from λ_g using initial guess values of ε and μ for the sample, we get:

$$\varepsilon_r = \mu_r\frac{(1-\Gamma)^2}{(1+\Gamma)^2}\left(1 - \frac{\lambda_o^2}{\lambda_c^2}\right) + \frac{\lambda_o^2}{\mu_r\lambda_c^2} \tag{48}$$

where ε_r and μ_r are initially guessed permittivity and permeability respectively, γ is propagation constant of material, c is velocity of light and f is frequency of incident EM radiation.

3.4. Shielding material and design considerations

The careful analysis of theoretical shielding expressions revealed that in order to meet design requirements and for extending efficient shielding action, shield should possess a balanced combination of electrical conductivity (σ), dielectric permittivity (ε) and magnetic permeability (μ) and physical geometry (Chung, 2001; Joo & Epstein, 1994; Saini, 2009a). Further, as shown in Fig. 1, the primary mechanism of EMI shielding is reflection from the front face of the shield, for which the shield must possess mobile charge carriers (electrons or holes) that can interact with the electromagnetic fields to cause ohmic (heating) losses in the shield. As a result, the shield needs to be electrically conducting, although only moderate conductivity (10^{-3} to 1.0 S/cm) is sufficient (Olmedo et al, 1997; Saini, et al 2011). The secondary EMI shielding mechanism is absorption for which shield should possess electric and/or magnetic dipoles which can interact with the electromagnetic fields in the radiation.

Metals are by far the most common materials for EMI shielding (Ott 2009; Paul 2004; Schulz et al, 1988) owing to their high electrical conductivity. In principle, for a highly conducting material (e.g. metals like Cu, Ag or Ni), only conductivity (σ) and magnetic permeability (μ) are important, such that the reflection loss (SE_R) is dependent upon their ratio (i.e. σ/μ) whereas the absorption loss (SE_A) is a function of their product (i.e. $\sigma.\mu$) [Chung, 2001; Joo & Epstein, 1994; Ott, 2009, Saini et al, 2011). However, in the case of moderately conducting materials permittivity (ε) also plays a significant role (besides σ and μ) in deciding absolute values of SE_R and SE_A . Such compounds are capable of displaying dynamic dielectric and/or magnetic loss, upon impingement by incident electromagnetic waves (Abbas et al, 2005, 2006; Joo & Epstein, 1994; Olmedo et al, 1997). Nevertheless, metal based compositions are suffered from problems (Ott, 2009; Paul, 2004; Saini et al, 2009a, 2009b) such as high reflectivity, corrosion susceptibility, weight penalty and uneconomic processing. Among other alternatives, carbon based materials (graphite, expanded graphite, carbon black, carbon nanotubes and graphene) have also been widely explored for possible applications in EMI shielding (Chung 2000, 2001, Gupta & Choudhary, 2011; Huang et al, 2006; Joo et al 1999, Makeiff & Huber, 2006; Pandey et al, 2009; Saini et al 2007, 2009a, 2009b, 2010, 2011; Singh et al, 2011; Yang, 2005a, 2005b). However, graphite exhibit poor dispersibility and high percolation threshold (Friend, 1993; Olmedo, 1997; Saini, 2009a). Similarly, CNTs are economically non-viable, difficult to produce at bulk scale and often require purification, auxiliary treatment and functionalization steps (Bal, 2007; Olmedo, 1997; Saini, 2009a, 2011). In this regard, intrinsically conducting polymers (ICPs) with tunable electrical conductivity/dielectric properties, facile processing and compatibility with other polymeric matrices can offer an attractive solution over other conducting fillers (Chandrasekhar, 1999; Ellis, 1986; Olmedo, 1997; Skotheim, 1986; Trivedi, 1997). Interestingly, due to their inherent electrical conductivity and dielectric properties, these ICPs can be used either as conducting

filler for various insulating matrices or as an electrically conducting matrix with incorporated conducting/dielectric/magnetic inclusions.

3.4.1. Intrinsically conducting polymers (ICPs)

Intrinsically conducting polymers (ICPs) combine moderate conductivity, good compatibility and ease of processability (as compared with carbons) with low density (~ 1.1–1.3 g/cm^3 compared to metals e.g. ~9.0 g/cm^3 for copper) and corrosion resistance (compared to metals) (Baeriswyl, 1992; Chandrasekhar, 1999; Ellis, 1986; Freund & Deore, 2007; Heeger, 2001a, 2001b; Joo & Epstein, 1994; MacDiarmid, 2001; Nalwa, 1997; Olmedo, 1997; Saini, 2011, Shirakawa, 2001; Skotheim, 1986; Trivedi, 1997). They possess unique shielding mechanism of reflection plus absorption rather than dominated reflection for metals and carbons. The ability to regulate their electrical conductivity by controlling parameters such as oxidation state, doping level, morphology and chemical structure, makes them powerful candidate for various techno-commercial applications. Fig. 6 shows the structure of some of the well known conducting polymers in their undoped forms.

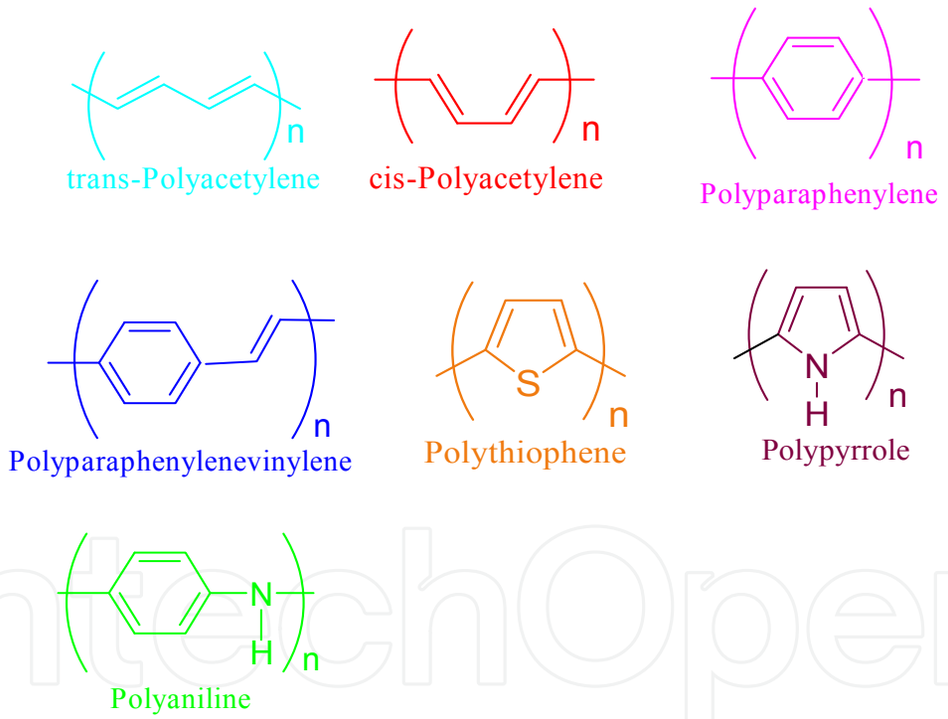

Figure 6. Chemical structures of some undoped conjugated polymers

Since the first ICP, polyacetylene (PA), was successfully synthesized by Shirakawa et al. (1977) and Chiang et al (1977, 1978a, 1978b) with conductivity as high as 10^6 S/cm in doped form, great interest has been aroused and a series of ICPs such as polyaniline (PANI), polypyrrole (PPY), polythiophene (PTH), poly(p-phenylene-vinylene) (PPV) etc have been developed (Carter et al, 1985; Rahman et al, 1989; Saxman et al, 1985; Snow, 1981; Soga et al, 1983; Thomas et al, 1988; Yamamoto et al, 1988). These undoped polymers display poor conducting properties and lies in insulating or semiconducting range (10^{-10} to 10^{-5} S/cm) as

shown in (Fig. 7). However, the controlled doping can transforms the poorly conducting undoped material into a system which displays semiconducting or metallic conductivity (10^{-6} to 10^{5} S/cm). The predicted theoretical value for highly doped PA is about 2×10^{7} S/cm, which is even higher than that of copper (Chiang et al, 1978a, 1978b). However, the highest experimentally recorded conductivity for PA (in highly oriented thin films form) was greater than 10^{5} S/cm, which is still the highest value that has been reported for any conducting polymer till date. In contrast, conductivity of other conjugated polymers reaches a maximum value ~10^{3} S/cm (Baeriswyl, 1992; Cao et al, 1992, 1995; Chaing et al, 1978a, 1978b; Chandrasekhar, 1999; Ellis, 1986; Heeger, 2001a; Nalwa, 1997; MacDiarmid, 2001; Shirakawa, 2001; Skotheim, 1986).

The display of metal like electrical and optical properties by the highly doped forms of these ICPs (synthetic polymers) also entitled them to be called synthetic metals (Freund & Deore, 2007; Heeger, 2001a, 2001b; Nalwa, 1997; MacDiarmid, 2001; Shirakawa, 2001; Skotheim, 1986). The intrinsic conductivity of conjugated polymers in the field of microwave (100 MHz – 20 GHz) makes them a viable shielding material. In particular, dependence of their conductivity on frequency, has inspired many scientific ideas to adopt these phenomenon to microwave applications (Coleman & Petanck, 1986; Karasz et al, 1985; Natta et al, 1958; Olmedo, 1995, 1997; Saini et al, 2009a, 2011).

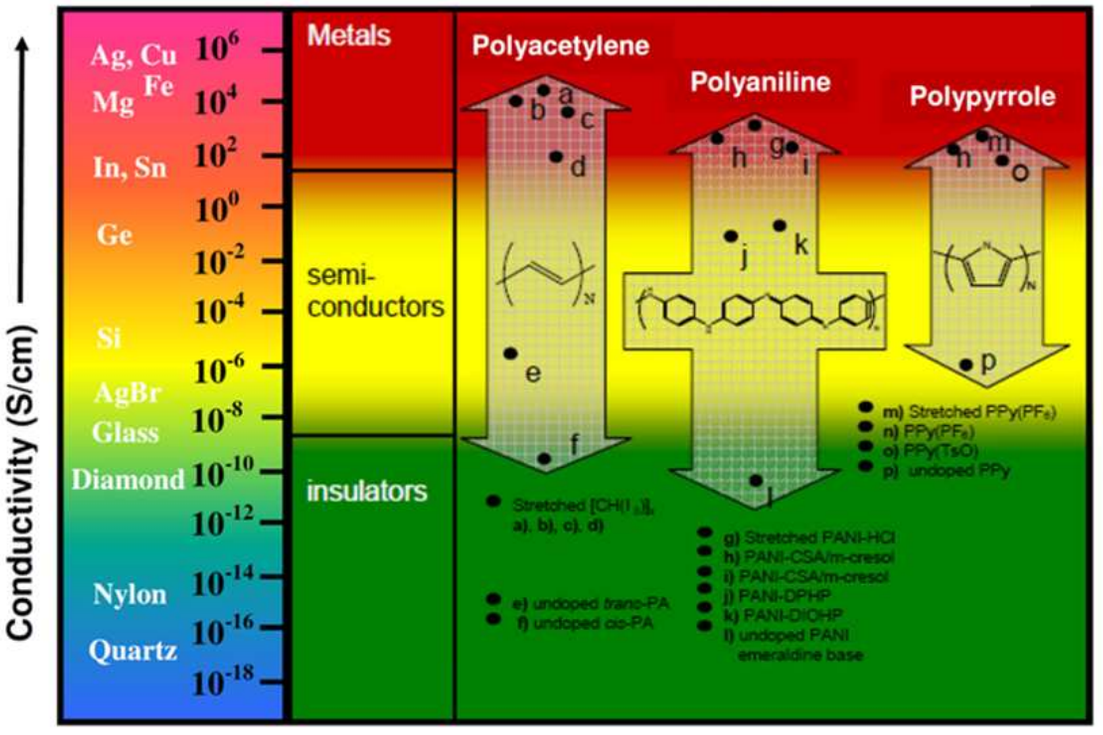

Figure 7. Conductivity of some conjugated polymers in comparison to typical metals, semiconductors or insulators.

The unique properties like tunable conductivity (between insulating and metallic limits), adjustable permittivity/permeability via synthetic means, low density, non-corrosiveness, nominal cost, facile processing (melt or solution), and controllable electromagnetic

attributes, further strengthen their candidature as futuristic shielding material for various techno-commercial applications. Their utility can also be extended to high-tech areas like space, defense (military), or navigation/communication control or as a radar absorbing material (RAM) in the stealth technology (Ellis, 1986; Knott et al, 1993; Olmedo, 1997; Nalwa, 1977). Especially, conducting polymers appear to be one of the few materials capable of displaying dynamic (switchable) microwave absorption behavior, which are called "intelligent stealth materials", due to the reversible electrical properties of conducting polymers affected by redox doping/de-doping processes.

A careful comparison of properties of large number of available shielding materials revealed that no single phase material can take care of all the aspects of shield (e.g. absorption coefficient, thickness, volume, broadband response) to give desired level of performance under different environments and applications. Therefore, several attempts have also been made to exploit the worthy property of above materials by making strategic combinations e.g. admixtures, blends and composites (Ajayan et al, 2000; Cao et al, 1992, 1995; Chung, 2000, 2001; Colaneri et al, 1992; Dhawan, 2003; Gangopadhyay et al, 2001; Grimes, 1994; Gupta & Choudhary, 2011; Huang et al, 2000; In et al, 2010; Joo et al, 1999; Koul et al, 2000; Liang et al, 2009; Pomposo, 1999; Ramanathan et al, 2008; Saini et al, 2009a, 2009b, 2011; Sanjai et al, 1997; Shacklette et al, 1992; Shi & Liang, 2008; Singh et al, 2011; Stankovich et al, 2006; Taka, 1991; Varrla, 2011; Wang & Jing, 2005; Wessling, 1999; Wojkiewicz et al, 2003; Zhang et al, 2011). Among these options, composites based on various organic/inorganic filler (guests) loaded ICP matrices (hosts) as well as ICP (guest) loaded insulating matrices (hosts) have captured maximum attention due to fascinating properties and wealth of prevalent applications (Chandrasekhar, 1999; Ellis, 1986; Freund & Deore, 2007; Heeger, 2001a, 2001b; MacDiarmid, 2001; Nalwa, 1997; Shirakawa, 2001; Skotheim, 1986). Recently, the discovery of various nanomaterials (NMs) and ability to design and tailor their electrical and electromagnetic properties has lead to scientific surge to identify the best materials for shielding and other applications (Ajayan et al, 1994; Alexandre, 2000; Baughman et al, 2002; Geim & Novoselov, 2007; Geim, 2009; Ijima, 1991; Meyer et al, 2007; Moniruzzaman & Winey, 2006; Rozenberga & Tenn, 2008; Stankovich et al, 2006, 2007; Thostenson et al, 2005). Especially, nanocomposites have attracted enormous scientific attention due to distinguished set of properties as well as promising applications.

3.4.2. ICP based nanocomposites

Nature has the astonishing ability to form self-organized functional nanomaterials with perfect structures and unusual properties e.g. bacteria, viruses, proteins, cells etc. which ordinarily falls in the size range of 1-100 nm (1 nm = 10^{-9} m). In fact, nature is considered as maestro nanotechnologist who has created one of the best known nanocomposites such as bones, hairs, shells, and wood. Therefore, in quest of making perfect nanocomposites, researches are trying to learn and mimic the natural material synthesis principles. However, though high quality bulk composites (e.g. straw reinforced mud, concrete, carbon/glass fiber reinforced polymers) were already realized by researchers, formation of perfect

nanocomposite remained a biggest scientific challenge. In case of nanocomposites, fillers possess nanoscale dimensions (~10^4 times finer than a human hair) and extend ultra-high interfacial area per volume to host polymeric matrices. Consequently, marked differences in the properties of nanocomposites are observed compared to their bulk counterparts e.g. enhanced strength, better optical or electrical properties etc. (Ajayan et al, 1994; Alexandre, 2000; Choudhary & Gupta, 2011; Mathur et al, 2010; Moniruzzaman & Winey, 2006; Ramasubramaniam, 2003; Rozenberga & Tenn, 2008; Thostenson et al, 2005) even at the lower loadings. Polymer is a versatile choice as a matrix material due to advantages like low density, mechanical flexibility, facile processing and corrosion resistance. Interestingly, most polymeric matrices possess poor electrical, dielectric or magnetic properties and are transparent to electromagnetic radiations (Saini et al, 2009a, 2011). Therefore, most of the electrical and electromagnetic properties of the conventional nanocomposites are mainly contributed by the nanofillers (nature and concentration) and matrix simply plays the role of holding the filler particles. In this consideration, utilization of ICPs as host matrix can offer an attractive solution over conventional (insulating) polymer based matrices (Ellis, 1986; Nalwa, 1997; Olmdo, 1995, 1997; Saini et al, 2011) primarily due to microwave non-transparency and design flexibility. However, the incorporation of nanofillers within polymeric matrices is not a straightforward task because of the ultrahigh surface area and agglomeration tendencies. These often resulted in failure to efficiently translate the nanoscopic properties of these fillers into macroscopic properties of resultant nanocomposites, thereby inability to utilize their full potential. Hence, handling and dispersion of nanofiller is the biggest challenge for nanocomposite science and technology.

3.4.3. Synthesis of ICP based nanocomposites

i. ICP as filler

As already mentioned in the previous section, inherent electric conductivity/dielectric properties (i.e. without any added conducting additive e.g. metals, graphite or carbon nanotubes), design flexibility and good compatibility with various insulating polymer matrices (e.g. thermoplastic/thermoset/rubber/elastomer/fiber/fabric etc.), ICPs can be used as filler to form composites.

As shown in Fig. 8, such composites are formed either by solution processing or by melt phase mixing/blending (Pud et al, 2003; Cao et al, 1992, 1995; Colaneri & Shacklette, 1992; Taka, 1991; Shacklette et al, 1992; Saini, et al, 2011; Wessling, 1999). In the former case both ICP and matrix polymer are dissolved/dispersed in a common solvent and stirred/sonicated to achieve the final mixing followed by casting (shaping) and drying/curing. In contrast, melt blending involves mixing of filler particles with molten matrix polymer followed by molding (shaping) and cooling/curing. In some case e.g. thermosts, ICPs are mixed with pre-polymer (resin) by solution blending technique. Finally, cross-linkers (curing agents) are added and curing is achieved by a combination of heat (not required for room temperature cross-linkers) and pressure (not required when no volatiles are expelled during curing process).

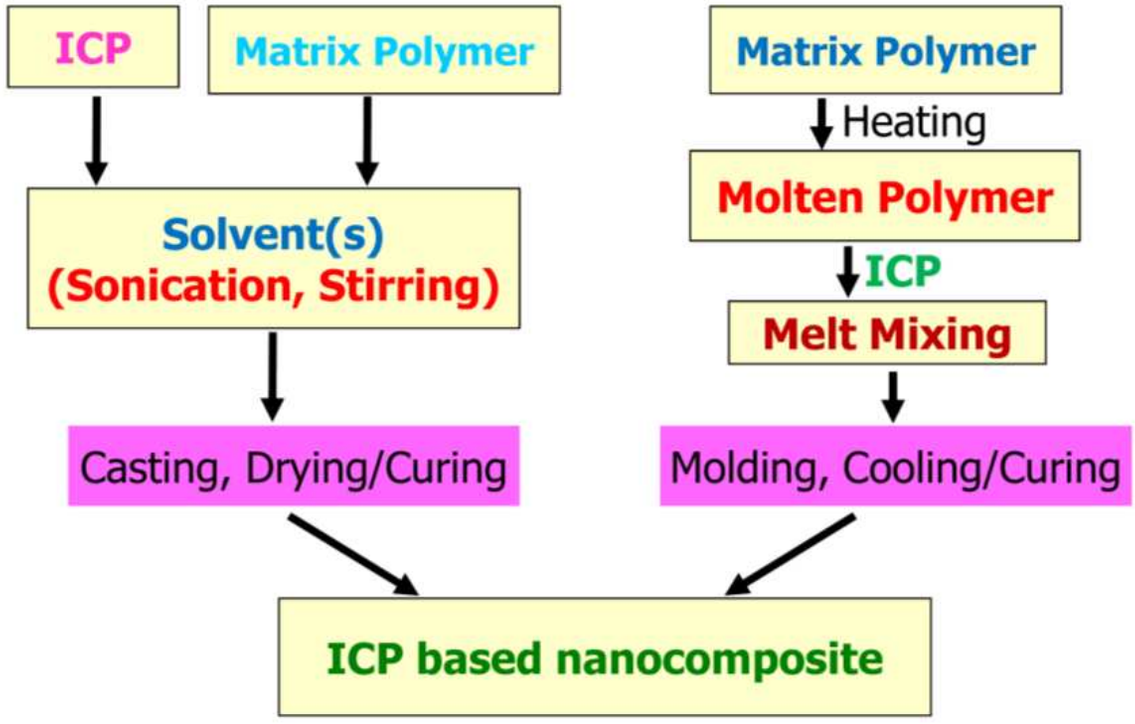

Figure 8. Schematic representation of steps involved in the formation of ICP (as conducting filler) loaded insulating polymer matrix by solution and melt processing techniques

ii. ICP as matrix polymer

The utilization of different ICPs as nanocomposite matrix can be attributed to advantages as design flexibility, good filler incorporation-ability, specific interactions with fillers and microwave non-transparency.

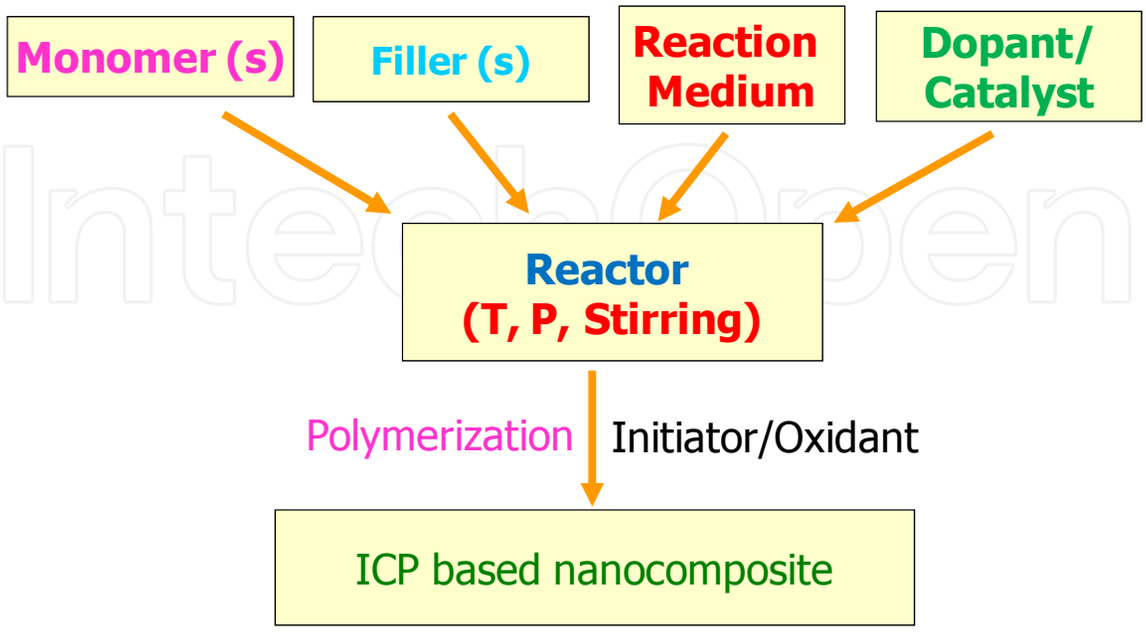

Figure 9. Schematic representation of formation of mechanism of ICP matrix based nano-composites by in-situ polymerization route.

The incorporation of various conducting, dielectric or magnetic nanoparticles within conducting polymer matrices can be achieved either by ex-situ physical mixing processes or by in-situ polymerization (Abbas et al, 2005, 2006; Das & Mandal, 2012; Dong et al, 2008; Fang et al, 2006; Joo et al, 1999; Moniruzzaman & Das, 2010; Pant et al, 2006; Phang et al, 2007, 2008; Saini et al, 2007, 2009a, 2009b, 2010; Yang et al, 2010, 2011). However, ex-situ mixing leads to poor dispersion of filler particles and failure to overcome their agglomeration tendencies that results in inferior and non-reproducible electrical and electromagnetic attributes. In contrast, the electronic properties of such synthetic metals can be strictly controlled by following in-situ incorporation (Fig. 9) approach i.e. carrying out the polymerization under the controlled conditions and in the presence of specific dopants and fillers (Bredas et al, 1998; Chandrasekhar et al, 2002, Mattosso et al, 1994; Nalwa et al, 1997; Saini et al, 2007, 2009a, 2009b; Savitha et al, 2005; Skotheim, 1986). In a typical reaction, monomer(s), filler and dopant or catalyst are charged into a suitably designed reactor to maintain required temperatre (T), pressure (P) and agitation (stirring) conditions. During such pre-polymerization process, monomers are generally adsorbed over dispersed nano-filler particles. The polymerization was initiated by addition of specific initiator/oxidant and allowed to proceed till reaction gets completed leading to formation of ICP based nanocomposite.

3.4.4. Electrical properties of ICP based nanocomposites

As already mentioned and shown in Fig. 1, the primary shielding mechanism is reflection for which shield should possess free charge carriers (electrons/holes) that can interact with incident EM field. But the organic conjugated polymers are insulators in their undoped forms e.g. room temperature electrical conductivity (σ_{dc}) of emeraldine base (EB) is ~10^{-9} S/cm (Fig. 10, Gupta et al, 2005). However, controlled doping leads to enhancement of conductivity due to formation of charge carriers (Fig. 11) i.e. polarons/ bipolarons (Saini et al, 2008; Stafstrom et al, 1987; Trivedi, 1997; Zuo et al, 1989) that can move under the influence of external potential and in the Coulmbic field of counter-ions distributed along the chain.

Therefore, increasing dopant concentration leads to increase in concentration and mobility of proto-generated charge carriers resulting in enhancement of conductivity. Furthermore, such a conductivity enhancement in conductivity is strongly dependent on nature and concentration of dopant and in some case conductivity well exceeds the required limit (Olmedo et al, 1997; Saini et al, 2011) for exhibiting good shielding effectiveness.

The addition of ICPs particles (guests) as a conducting filler within insulating polymer matrices (hosts) leads to establishment of electrical conductivity (in resultant nanocomposites) due to formation of percolation networks (Colaneri & Shacklette, 1992; Hsieh, 2012; Lakshmi et al, 2009; Shacklette et al, 1992; Taka, 1991; Wessling, 1999). At percolation threshold, ICP particles form a 3D conductive network within host matrix, which can be easily estimated by plotting the electrical conductivity as a function of the reduced volume fraction of filler (Fig. 9) and performing data fitting with a power law function (Saini et al, 2011):

$$\sigma = \sigma_o \left(v - v_c\right)^t \tag{49}$$

where σ is the electrical conductivity of the composite, σ_o is characteristic conductivity, v is the volume fraction of filler, v_c is volume fraction at the percolation threshold and t is the critical exponent. The log (σ) versus log ($v - v_c$) plot (Fig. 12) gives a straight line according to eqn. 10. The values of scaling law parameters i.e. v_c and t can be subsequently obtained by least-square analysis of the above double logarithmic plots. When the densities of the host polymer and the filler are similar, mass fraction (m) becomes same as volume fraction (v) and can be used in above calculations.

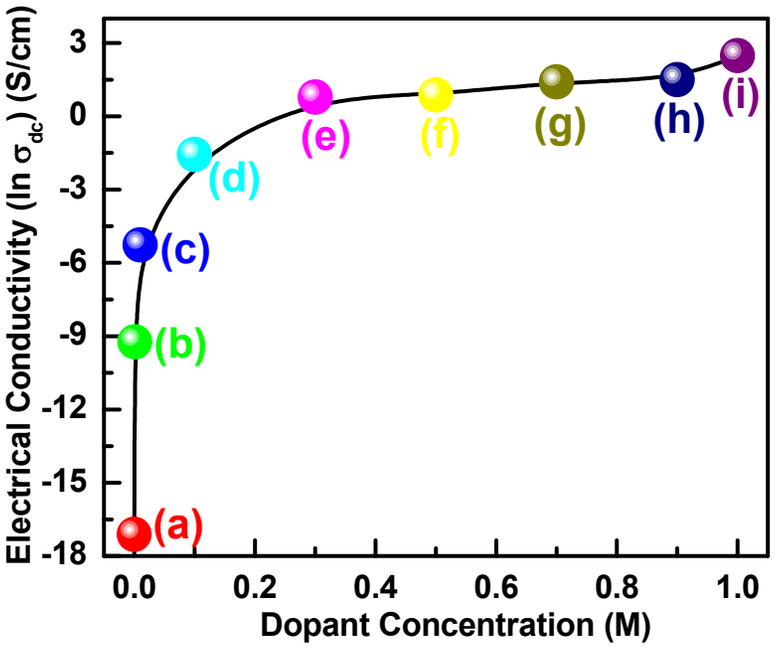

Figure 10. Variation of electrical conductivity (ln σ_{dc}) of hydrochloric acid (HCl) doped Emeraldine base (EB) samples as a function of dopant (HCl) concentration (a) 0.0 M (b) 0.001 M, (c) 0.01 M, (d) 0.1 M, (e) 0.3 M, (f) 0.5 M, (g) 0.7 M, (h) 0.9 M and (i) 1.0 M.

However, it has been observed that formation of such networks and percolation thresholds (minimum loading level at which first continuous network of conducting particles is formed) critically depend on nature of ICP, its intrinsic conductivity, particle shape, morphology, aspect ratio, its concentration, degree of dispersion and extent of compatibility with host matrix.

Nevertheless, at percolation conductivity (σ_p) remained too low to exhibit any acceptable shielding action and generally higher loadings (>30 wt. %) are required though in most cases, σ_p is sufficient to extend antistatic action. Interestingly, when ICPs are combined with other conducting fillers (e.g. Polyaniline with MWCNT, Saini et al, 2011) significant reduction in percolation threshold, higher conductivity and better shielding performance is observed as compared to pristine (unfilled) ICPs.

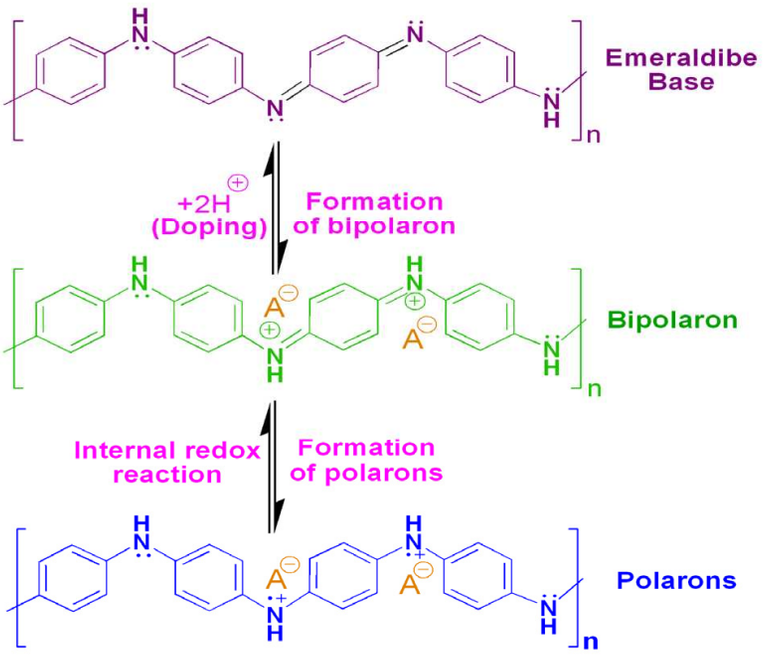

Figure 11. Protonic acid doping of polyaniline leading to formation of charge carriers polarons (radical cations) and bipolarons (dications)

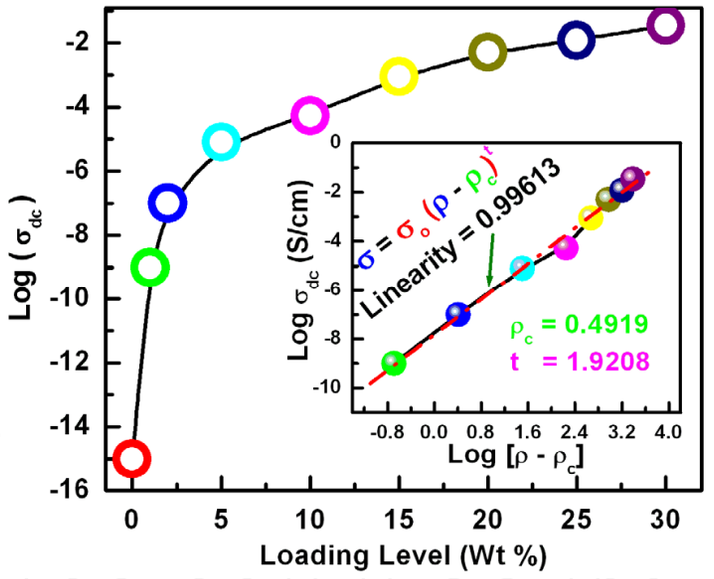

Figure 12. Variation of conductivity (σ_{dc}) of PANI-MWCNT nanofiller loaded polystyrene solution blends. Inset shows the percolation and scaling details

In many cases conjugated polymers are used as matrix instead of conventional insulating polymers. When conducting fillers (e.g. metal particles, carbon black, graphite or CNTs) are incorporated within undoped (poorly conducting) ICP matrices, electrical conductivity increases and follows a typical percolation behavior. In contrast, the loading of above conducting fillers within microwave non-transparent doped (intrinsically conducting) ICP matrices lead to further enhancement (Fig. 13) of electrical conductivity. Such improvement can be explained on the basis of granular metal/inhomogeneous doping model (Sheng &

Klafter, 1983) which considered that ICPs consists of highly conducting metallic islands dispersed within low conductivity amorphous matrix. Therefore, above improvement in conductivity can be attributed to bridging of these metallic islands (Saini et al, 2009a) by the metallic filler particles facilitating enhanced inter-particle transport. The increase in conductivity is strongly dependent on nature, concentration and aspect ratio of filler particles as well as type and morphology of host ICP matrix.

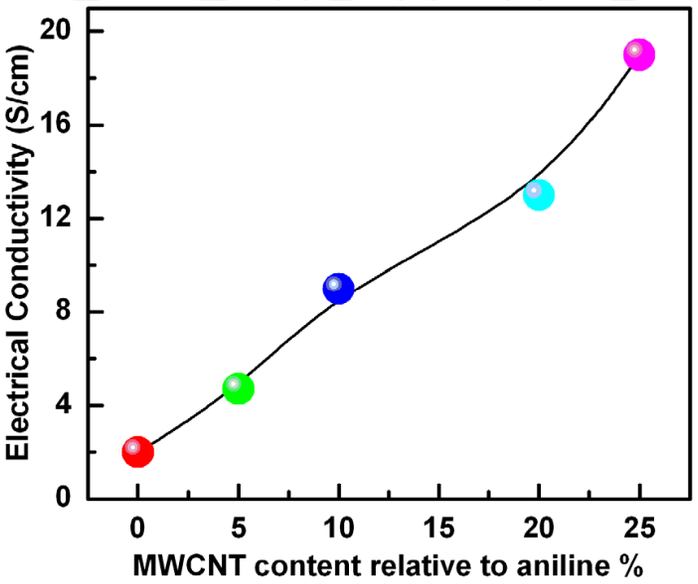

Figure 13. Dependence of electrical conductivity of in-situ polymerized PANI-MWCNT nanocomposites on MWCNT content

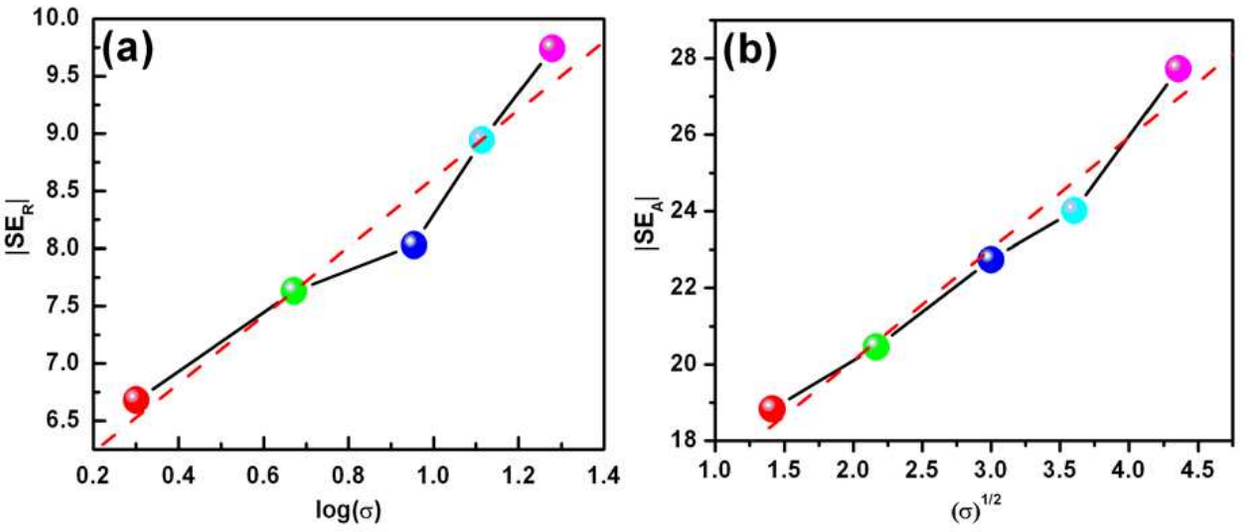

Figure 14. Correlation between electrical conductivity (σ) and shielding effectiveness (SE) showing linear dependences of (a) reflection loss (SE_R) on log σ and (b) absorption loss (SE_A) on $\sigma^{1/2}$.

Nevertheless, the establishment and enhancement of electrical conductivity is of paramount importance because it leads to parallel enhancement of reflection and absorption loss components (Fig. 14, Saini et al, 2009a) leading to enhancement of overall shielding

effectiveness. Interestingly, absorption loss (SE_A) increases by much larger magnitude (with conductivity) compared to corresponding reflection loss (SE_R) component. For a non-magnetic material, this can be explained on the basis of logarithmic [i.e. log(σ)] and square root [i.e. $(\sigma)^{1/2}$] conductivity dependence of SE_R and SE_A respectively as shown in Fig. 14.

3.4.5. Dielectric and magnetic properties of ICP based nanocomposites

A secondary mechanism of shielding is absorption for which shield should possess electric or magnetic dipoles. These dipoles can interact with transverse electric (E) and magnetic (H) vectors of the incident EM waves to introduce losses into the system. It is interesting to note that pure (without any external filler loading) conjugated polymers in their undoped (base) forms possess poor dielectric and magnetic properties. However, controlled doping leads to marked improvement (Fig. 15) in dielectric properties (e.g. dielectric constant/real-permittivity, dielectric losses/imaginary-permittivity), although even after doping magnetic properties (e.g. real and imaginary magnetic permeability) remained poor.

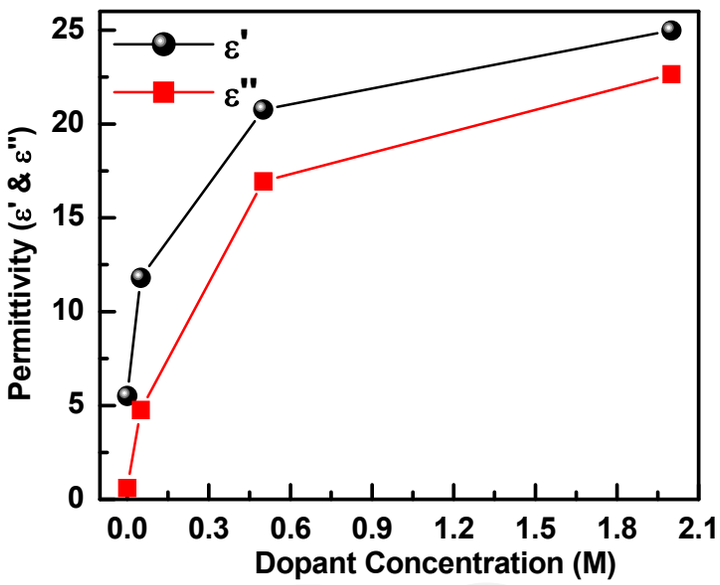

Figure 15. Dependence of (a) real permittivity or dielectric constant (ε') and (b) imaginary permittivity or dielectric loss (ε'') on the dopant concentration for acrylic acid (AA) doped emeraldine base (EB) samples

As already discussed, doping of ICPs leads to formation of polarons/bipolarons (Fig. 11) that produces pronounced polarization/relaxation effects (Olmedo et al, 1995, 1997; Saini et al, 2008, 2009a, 2011; Stafstrom et al, 1987). Therefore, observed improvement of dielectric properties with doping level can be attributed formation and increase in concentration of above localized carriers. The correlation between dielectric properties and shielding response for various ICPs is presented in Fig.16 which clearly shows that the total shielding efficiency (SE_T) increases as the absolute value of complex dielectric constant increases.

The increase of both real and imaginary parts of dielectric permittivity contributes (Joo & Epstein, 1994) towards enhancement of SE_T. Furthermore, the complex dielectric constant

dependence of absorption loss (SE_A) component (inset of Fig. 16) was found to be much stronger compared to that due to reflection loss (SE_R). In some cases, especially for highly doped and stretch oriented ICPs; dielectric constant becomes negative (Javadi et al, 1989; Joo & Epstein, 1994; Joo et al, 1994; Hsieh et al, 2012; Wang et al, 1991) and ultra-high attenuation is observed which suggests the possibility of ICP based left handed materials (LHMs) or meta-materials.

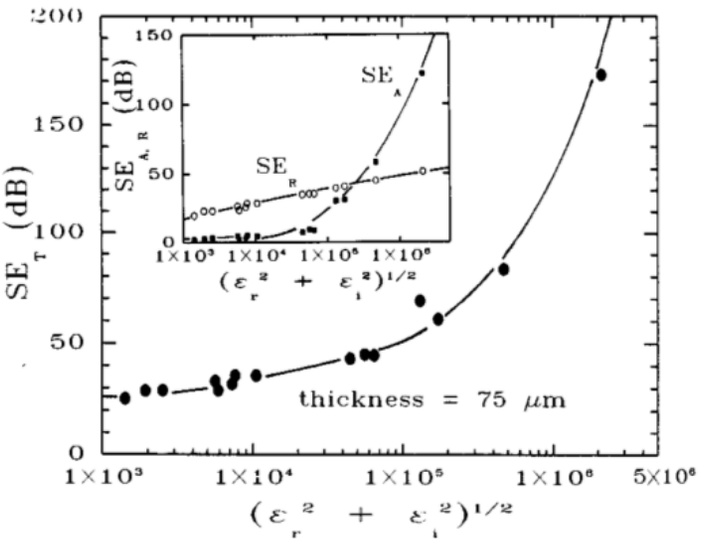

Figure 16. Total shielding efficiency (SE_T) vs absolute value of complex dielectric constant [$(\varepsilon_r^2 + \varepsilon_i^2)^{1/2}$] of various conducting polymers. Inset: comparison of reflection (◦) and absorption (▪) shielding efficiency as a function of absolute value of complex dielectric constant. Solid lines are guides to the eye. Reprinted with permission from [J. Joo and A. J. Epstein, Appl. Phys. Lett. 65 (18), 2278-2280, 1994]. Copyright [1994], American Institute of Physics.

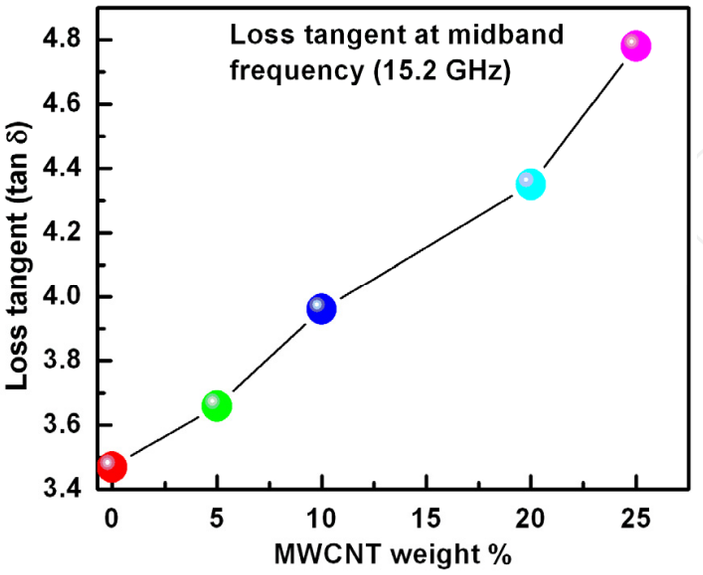

Figure 17. Loss tangent (tan δ) of in-situ synthesized PANI-MWCNT nanocomposites as a function of MWCNT loading

Interestingly, for ICPs, besides doping induced polarization filler induced interfacial polarization may also contribute towards dielectric properties. For example, when conducting fillers like metal particles, graphite or carbon nanotubes are introduced into ICP matrices; further improvement of dielectric properties was observed. Such a polarization occurs due to electrical conductivity differences between ICP and metallic fillers leading to charge localization at interfaces via Maxwell-Wagner-Sillars (Kremer & Schönhals, 2003; Riande & Diaz-Calleja, 2004; Sillars, 1937; Wagner, 1914) interfacial polarization phenomenon. Such polarization and related relaxation phenomenon contribute towards energy storage and losses. The actual losses can be computed by normalization of these losses with storage terms [i.e. by ratio of dielectric losses/imaginary permittivity (ε'') with dielectric constant/real permittivity (ε')] to quantity loss tangent (tan δ).

In case of in-situ formed MWCNT-polyaniline nanocomposites, improvement of dielectric properties leads to high value of loss tangent (Fig. 17) which further increases (Saini et al, 2009a) with increase in MWCNT loading. However, though for a given thickness, total shielding is dominated by absorption, reflection loss component becomes too high form the viewpoint stealth technology. Nevertheless, despite good dielectric properties, magnetic properties of ICPs remained poor to extend any significant contribution towards EMI regulation. In principle, for highly conducting materials, only conductivity (σ) and magnetic permeability (μ) are important, such that the reflection loss (SE_R) is dependent upon their ratio (i.e. σ/μ) whereas the absorption loss (SE_A) is a function of their product (i.e. σ.μ) (Saini et al, 2011). In contrast, for moderately conducting materials (e.g. ICPs) permittivity (ε) also plays a significant role (besides σ and μ) in deciding absolute values of SE_R and SE_A (Joo & Epstein, 1994). As most ICPs are non magnetic in nature ($\mu_r \approx \mu_i \approx 0$), observed attenuations are mainly governed by σ and ε only. Therefore, it is expected that any improvement in magnetic properties will lead to definite improvement of absorption loss alongwith parallel reduction of reflection loss. In addition, the incorporation of high dielectric constant materials like $BaTiO_3$, ZnO, TiO_2 etc. within ICP matrices are expected to further improve the microwave absorption response. Consequently, in recent years, lot of work has been carried out to formulate composites of polyaniline with the dielectric or magnetic filled inclusions, either by in-situ polymerization or by ex-situ physical mixing processes (Abbas et al, 2005, 2006, 2007, 2008). Such composites possess moderate polarization or/and magnetization alongwith good microwave conductivity so as to introduce absorbing properties into the material. They display dynamic dielectric and/or magnetic losses, upon impingement by incident electromagnetic waves. As electromagnetic wave consists of an pulsating (orthogonal to each other) electric (E) and the magnetic (H) fields; therefore, above multi-component composites are expected to yield good attenuation efficiencies, primarily due to interaction of conducting/dielectric and conducting/magnetic phases with E and H vectors of the incident EM waves (Fig. 5). Furthermore, most insulating polymer matrices possess poor electrical, dielectric or magnetic properties and are transparent to radio frequency (RF) or microwave (MW) electromagnetic radiations (EMRs). Therefore, only fillers contribute towards shielding and leakage of radiation from EMR transparent regions tends to degrade shielding effectiveness. However, microwave non-transparency (Olmedo et al, 1995, 1997; Saini et al, 2011) of ICPs compared to conventional polymers is an added

advantage as both filler and matrix contribute towards shielding. Moreover, the dominant shielding characteristic of absorption for above nanocomposites materials other than that of reflection for metals render ICPs more useful in applications requiring not only high EMI SE but also shielding by absorption, such as in stealth technology.

When ICPs are exploited as microwave non-transparent matrices, the added dielectric or magnetic filler particles result in establishment of properties (e.g. dielectric/magnetic character, thermal conductivity etc.), that are extrinsic to these intrinsically conducting polymers. Therefore, combination of dielectric or magnetic nanoparticles with conducting polymer leads to formation of multi-component composite possessing unique combination of electrical, dielectric and magnetic properties useful for suppression of electromagnetic noises and reduction of radar signatures (Abbas et al, 2005, 2007; Chan, 1999; Chandrasekhar, 1999; Cho & Kim, 1999; Dong et al, 2008; Ellis, 1986; Gairola et al, 2010; Huang, 1990; Knott et al, 1993; Kurlyandskaya et al, 2007; Meshram et al, 2004; Nalwa, 1997; Ngoma et al, 1990; Pant et al, 2006; Phang et al, 2007, 2008, 2009, 2010; Xiaoling et al, 2006; Xu et al, 2007; Yang et al, 2009). The incorporation of magnetic fillers (e.g. ferrites like γ-Fe_2O_3 or Fe_3O_4) within ICP matrices leads to improvement of magnetic properties (Fig. 18) without much loss of conductivity. Such a combination is expected to display additional magnetic loss leading to enhanced absorption.

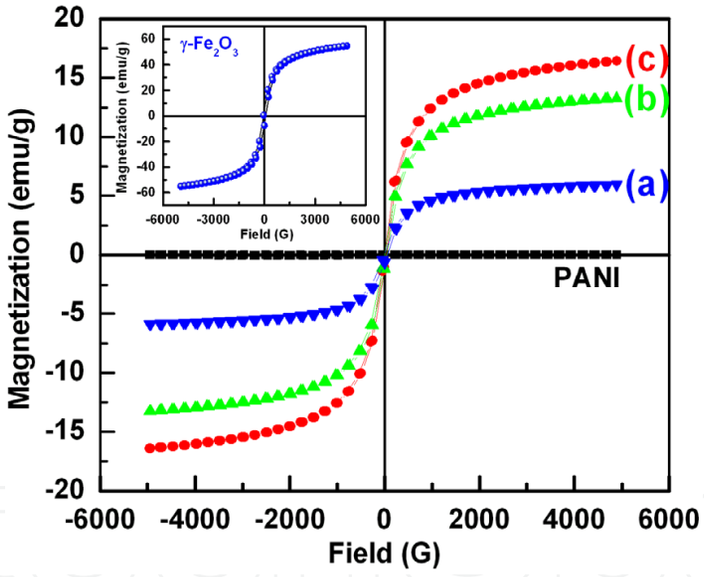

Figure 18. Magnetization of polyaniline (PANI), γ–Fe_2O_3 nanoparticles and nanocomposites formed by in-situ polymerization taking different weight ratio of aniline: γ–Fe_2O_3 (a) 2:1, (b) 1:1 & (c) 1:2

The magnetization plots (Fig. 18) of polyaniline/γ-Fe_2O_3 composites revealed that pure γ-Fe_2O_3 nanoparticles display pronounced magnetic signatures with narrow hysteresis loop. The saturation magnetization (M_s) value of of these particles was found to be 59.3 emu/g (at 5.0 kG) alongwith very small retentivity (M_r~ 4.3 emu/g) and coercivity (H_c~ 83.8 G), which indicate the super-paramagnetic (SPM) nature of these particles. The SPM character imparts fast relaxation behaviour and originates due to small size of the ferrite particles i.e. approaching towards the single domain limit (Qiao et al, 2009). However, PANI possesses weak ferromagnetic behaviour and with increase in ferrite content, enhancement of M_s was

observed with as parallel reduction of coercivity (H_c). The initial permeability (μ_i) of ferromagnetic materials can be expressed as (Stonier, 1991):

$$\mu_i = \left(\frac{M_s^2}{akH_cM_s + b\lambda\xi} \right) \tag{50}$$

where *a* and *b* are two constants determined by the material composition, λ is the magneto-striction constant, ξ is elastic strain parameter of crystal, and k is a proportionality coefficient. The above equation shows that permeability can be enhanced either by enhancing M_s or by reducing H_C. In the present system, the incorporation of ferrite within PANI matrix is expected to affects the surface electron density of γ-Fe_2O_3 nanoparticles and hence the spin-spin or spin-lattice interactions. The results show that M_s value increases (5.94 to 16.4 emu/g) with increasing ferrite content (plots a-c) whereas H_c shows a simultaneous decrement (35.7 to 57.8 G). Therefore, It can be seen from the eqn. (50) that both higher M_s and lower H_c values are favorable to the improvement of μ_i value, which in turn is expected to enhance the microwave absorption capability.

In many cases, highly doped ICP particles are used as conducting fillers (in place of metal or carbon based materials) for various insulating polymer host matrices. This not only leads to establishment and improvement of electrical conductivity but also contribute towards improvement of both real as well as imaginary permittivity (Abbas et al, 2005; Colaneri & Shacklette, 1992; Joo et al, 1994; Saini et al, 2011; Shacklette et al, 1992; Taka, 1991; Wessling, 1999).

Again the magnetic properties remained poor due to non-magnetic nature of most ICPs. However, when magnetic filler loaded ICPs is use hybrid filler, improvement in magnetic properties has also been observed besides regular improvement of dielectric attributes. For example use of PANI-MWCNT hybrid filler within polystyrene matrix leads to formation of composites with magnetic properties due to MWCNT core (containing entrapped ferromagnetic iron catalyst phase) and electrical conductivity/dielectric properties due to ICP and MWCNTs. As the concentration of PANI-MWCNT filler increases, real and imaginary parts of both permittivity and permeability increases as shown in Fig. 19. Most importantly, losses due to reflection (SE_R) and absorption (SE_A) follows the permittivity and permeability trends and exhibit corresponding increase. However, SE_A was more sensitive towards electromagnetic attributes compared to SE_R which may be attributed to their square root and logarithmic dependences. Furthermore, two most important parameters that decide the relative magnitudes of SE_R and SE_A are microwave conductivity (σ_T) and skin depth (δ). The σ_T can be related to imaginary permittivity (ε'' or ε_i) as (Saini et al, 2011):

$$\sigma_T = (\sigma_{ac} + \sigma_{dc}) = \omega\varepsilon_o\varepsilon'' \tag{51}$$

where σ_{ac} and σ_{dc} are frequency dependent (ac) and independent (dc) components of σ_T respectively, ω is angular frequency and ε_o is permittivity of free space (8.85×10^{-12} F/m). Higher the value of σ_T more will be reflection for a given absorption. Further, the skin depth (δ) of the shield is defined as depth of penetration at which strength of incident EM signal is

reduced to ~37% of its original magnitude. For a good conductor (i.e. $\sigma_T \gg \omega\varepsilon$), it (δ) can be expressed in terms of σT real permeability (μ' or μ_i) and ω as (Joo. et al, 1994):

$$\delta = \left(\frac{2}{\sigma_T \omega \mu'} \right)^{\frac{1}{2}} \tag{52}$$

Now shallower is the skin depth, higher will be absorption loss for a given thickness of material. Fig. 20 shows that as the loading level of PANI-MWCNT filler within PS matrix increases, σT increases whereas δ value decreases.

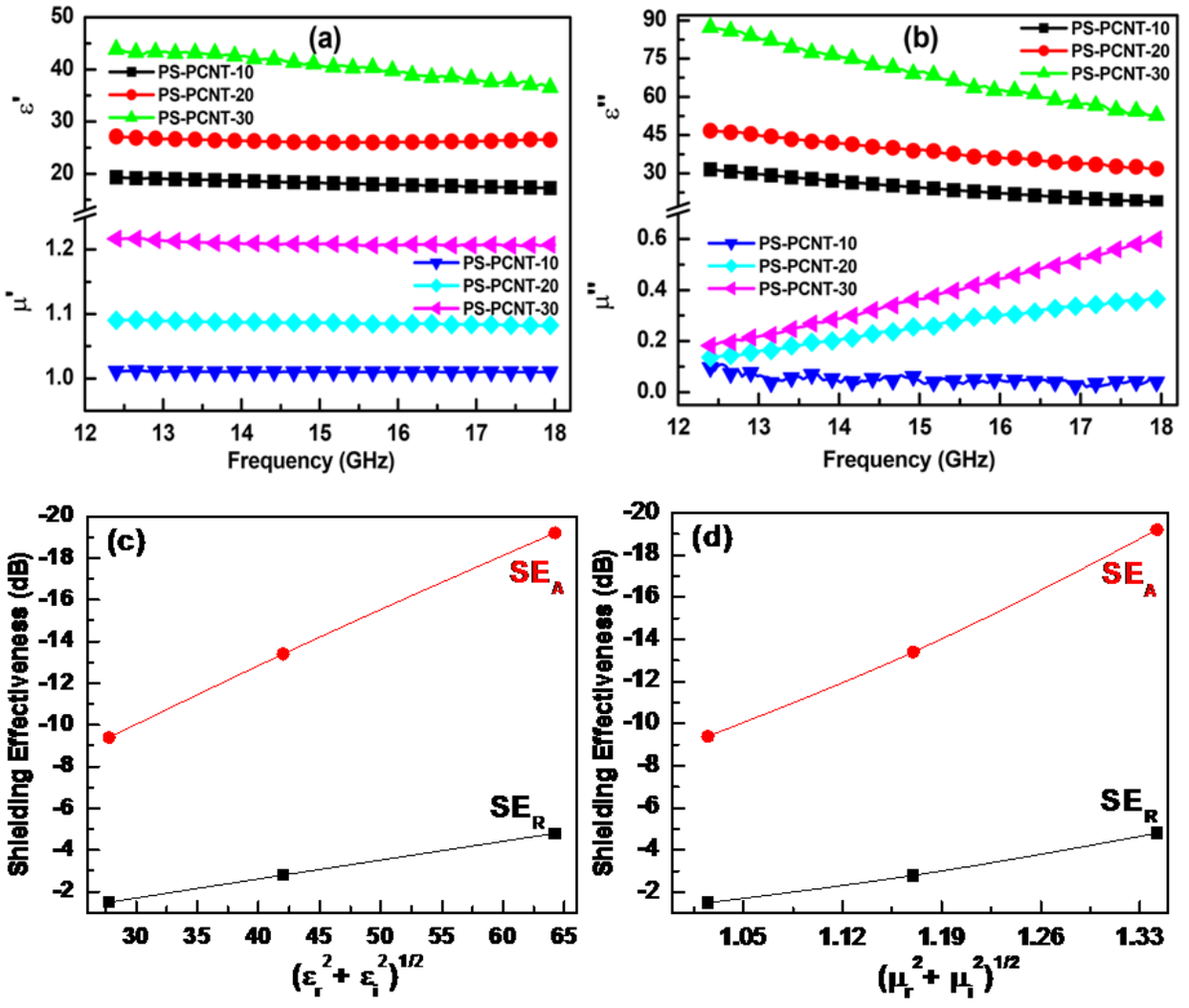

Figure 19. Frequency dependence of (a) dielectric constant (ε') & real permeability (μ'), (b) dielectric loss (ε'') & magnetic loss (μ'') of PANI-MWCNT/Polystyrene nanocomposites with increasing loading (10, 20 & 30 weight %) of PANI-MWCNT filler. Dependences of losses due to absorption (SEA) and reflection (SER) of above composites as a function of absolute value of (c) complex permittivity [($\varepsilon_r^2 + \varepsilon_i^2$)1/2] , (d) complex permeability [($\mu_r^2 + \mu_i^2$)1/2].

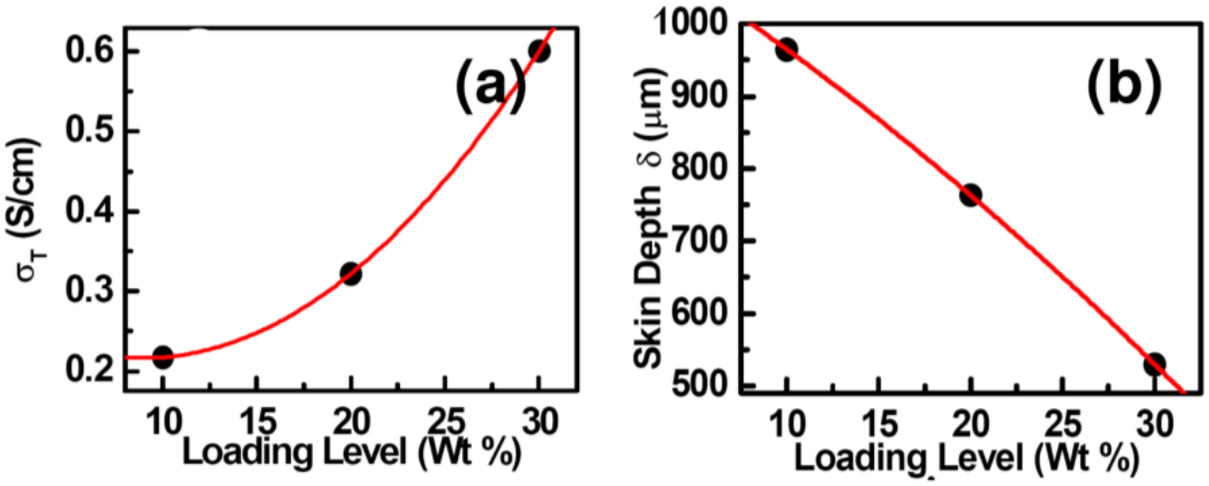

Figure 20. Dependence of (a) σ_T and (b) δ value of PANI-MWCNT loaded polystyrene composites on the loading of PANI-MWCNT

3.4.6. EMI shielding performance of ICP based nanocomposites

In the previous section we learned about the importance of parameters such as electrical conductivity and dielectric/magnetic attributes in regulating the shielding effectiveness and their correlation with reflection and absorption loss components. This section is devoted to measurement and interpretation of shielding effectiveness alongwith detailed analysis of reflection and absorption sub-components.

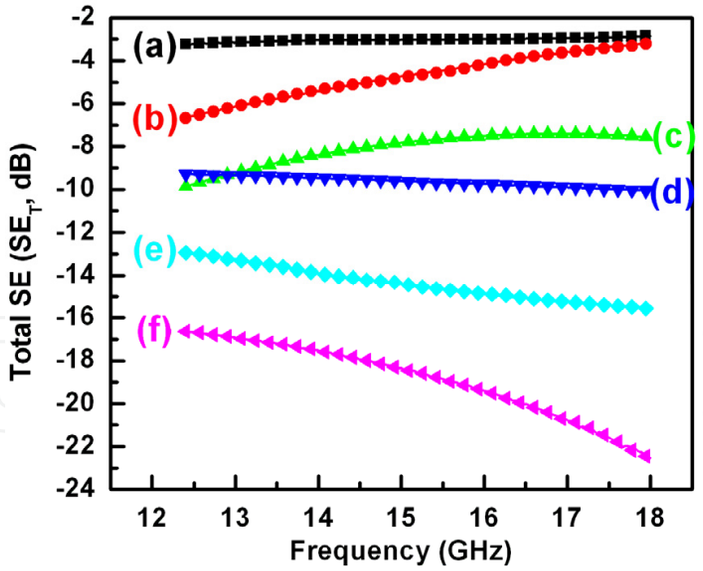

Figure 21. Frequency and dopant concentration dependence of total shielding effectiveness (SE_T) value of samples prepared by doping of emeraldine base (EB) with different concentrations of acrylic acid (AA) viz. (a) 0.0 M, (b) 0.05 M, (c) 0.1 M, (d) 0.5 M, (e)1.0 M and (f) 2.0 M

As already discussed doping produces localized defects (polarons/bipolarons) that are responsible for polarization and electrical conductivity. With the increase in dopant concentration, achieved doping level increases leading to enhancement of polaronic

concentration as well as related conductivity/permittivity, which ultimately leads to improvement of shielding effectiveness (Fig. 21). Nevertheless, though based on microwave dielectric constant and electrical conductivity values many speculations were made about the shielding properties of ICPs, the first direct evidence of shielding response of ICP based composites alongwith actual shielding effectiveness values was presented by Taka (1991). He prepared poly(3-octyl thiophene) composites by melt mixing chemically synthesized poly(3-octyl thiophene) with PS, PVC, and EVA in and tested for EMI shielding at frequency range from 100 kHz to 1GHz. EMI SE of these composites (3 mm thick) increased with the polymer loadings and -45 dB (from 100 kHz to 10 MHz) was achieved with high (i.e. 20%) loading in the PVC that was still lower than that of a nickel painted sample (-80 dB). The measurements showed that P3OT blends behave as pseudo-homogenous metals (PHM). A PHM has no intentional holes or slits but lacks homogeneity. The shielding efficiency depends strongly on the amount of conducting polymer mixed in the blends due to regulation of conductivity. The authors concluded that composites with 20% or less loading of poly(3-octyl thiophene) were not readily applicable as EMI shielding.

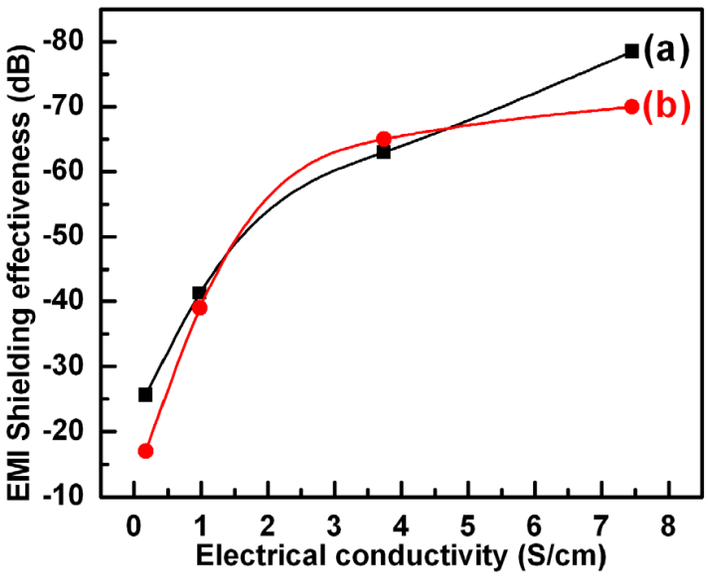

Figure 22. EMI shielding effectiveness (at 1.0 GHz frequency) of ICP loaded PVC blends as a function of DC electrical conductivity under (a) far field and (b) near field regimes

Later, systematic study of EMI shielding behavior of conducting polymer (PANI) based thermoplastic blends with polyvinyl chloride (PVC) or Nylon was reported (Colaneri & Shacklette, 1992; Shacklette et al, 1992). The EMI SE values of these highly conducting blends (~0.1-20 S/cm) were measured over a frequency range of 1 MHz to 3 GHz and also calculated theoretically under both near and far field regimes. The results are graphically presented in Fig. 22 which showed that both near and far filed SE followed the DC electrical conductivity and exhibit rapid initial rise followed by slow increment at higher conductivity. Far field SE of -70 dB was obtained for the melt blend of polyaniline (again at higher loading level of 30 wt. %) with PVC which agreed well with the theoretical calculations as per expressions derived by authors. Pomposo et al (1999) have prepared PPY based conducting hot melt adhesives by melt mixing appropriate amounts of ethylene-co-

vinyl acetate (EVA) copolymer and PPY, which was synthesized with oxidant of $FeCl_3$. Both near and far field EMI shielding properties of the adhesives were measured at room temperature and found to increase with the loading of PPY. Near field SE in excess of -80 dB was determined at 1MHz and above -30 dB at 300 MHz, though a decrease with increase of frequency. Far field SE values of -22, -27 and -30 dB were determined (in the 1 to 300 MHz frequency range) for PPY loadings of 15, 20 and 25% respectively. Similarly, Wessling (1999) prepared highly conductive blends of PANI with PVC, polymethylmethacrylate (PMMA) or polyester at Ormecon Chemie, with conductivities of ca. 20 S/cm and in some cases up to 100 S/cm. These blends exhibited EMI SE of -40 to -75 dB for both near and far field conditions. However, mechanical properties were not encouraging and demanded considerable improvement. In addition the higher necessary thicknesses of 2-3 mm of these blends were found to be higher than technically acceptable thickness of 0.5–0.8 mm for practical uses.

Naishadham & Kadaba (1991), Naishadham & Chandrasekhar (1998) and Chandrasekhar & Naishadham (1998) reported the cumulative broadband (4-18 GHz) measurements and computations of all microwave parameters (e.g. conductivity, absorption, complex permittivity, shielding and reflection) of sulfonate doped PANI. It was found that the total SE of -35 to -15 dB was obtained with return loss of -5 to -1 dB and nominal absorption of -5 dB for PANI samples of conductivity 1-7 S/cm. Authors also demonstrated that better SE value upto -50 dB can be realized by stacking several polymeric sheets of different thicknesses or by sandwiching a lossy dielectric between two sheets of the same thickness.

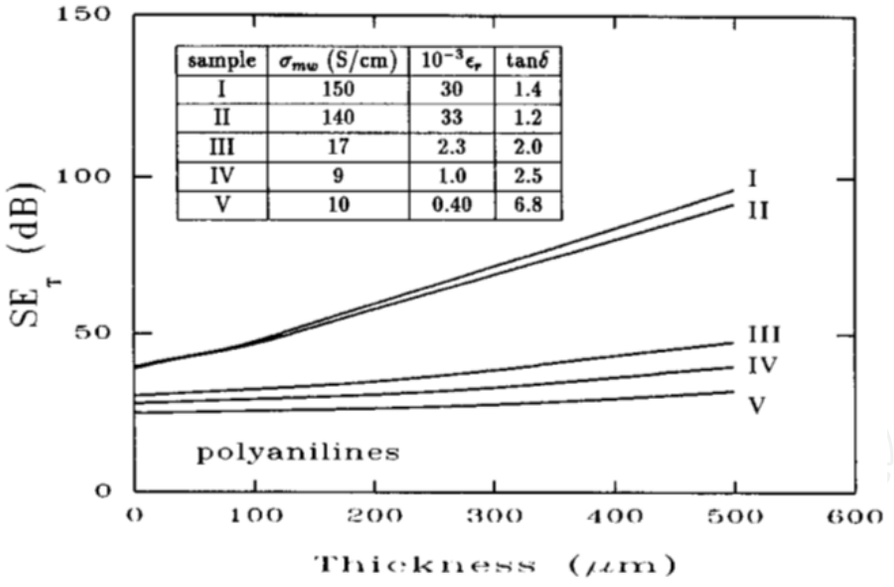

Figure 23. Thickness dependence of total shielding efficiency (SE_T) of various ''crosslinked'' polyaniline (XPANI-ES) samples. Sample I: highly XPANI-ES [3.5 times (×) stretched, parallel (||)], sample II: intermediate XPANI-ES [3.5×,||), sample III: highly XPANI-ES (3.5×, ⊥), sample IV: highly XPANI-ES (unstretched), and sample V: non-XPANI-ES (12.5×, ⊥). Inset: comparison of σ_{mw} , ε_r, and tan δ. Reprinted with permission from [J. Joo and A. J. Epstein, Appl. Phys. Lett. 65 (18), 2278-2280, 1994]. Copyright [1994], American Institute of Physics.

It has been found that electrical conductivity is not the sole scientific criteria for exhibiting high shielding effectiveness (Joo & Epstein, 1994) and good attenuations were also extended

by moderate conductors with good dielectric properties. In fact as mentioned in the previous section, it has now been established that shielding effectiveness increases (as shown previously in Fig. 16) with absolute value of complex dielectric permittivity. Furthermore, absorption loss was found to be more sensitive towards permittivity (inset Fig. 16) than corresponding reflection loss. Figures 23 and 24 show the microwave SE of pure ICPs including PANI and PPY (in thin film forms) as a function of their intrinsic properties (insets of Fig. 23 and Fig. 24) such as microwave conductivity (σ_{mw}) and dielectric constant (ε_r) alongwith its dependence on extrinsic parameters like thickness (t) and temperature (T). The role of parameters like degree of crosslinking and parallel (||) or perpendicular ($\perp$) stretch orientation which tends to affect σ_{mw}, ε_r or loss tangent (tanδ) has been clear from the table data (above insets).

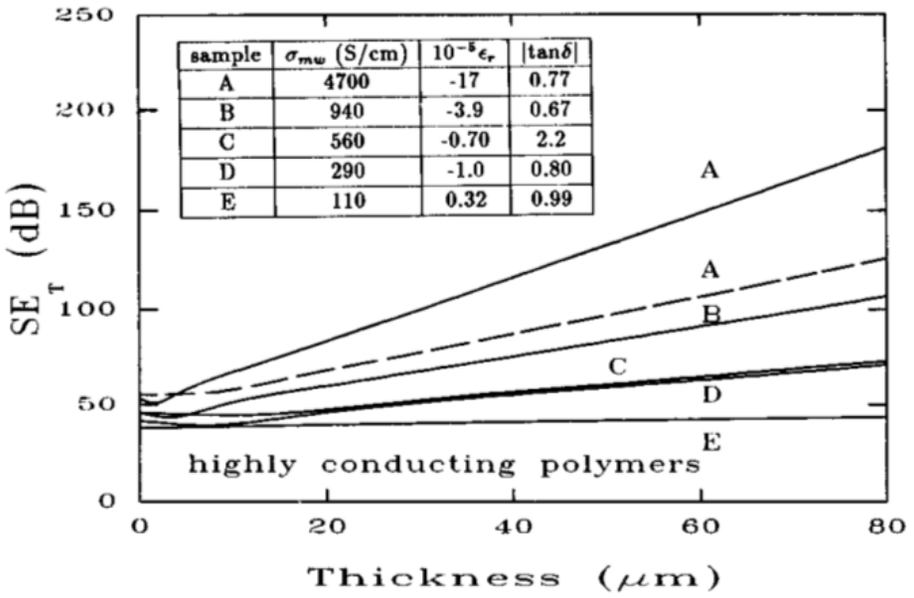

Figure 24. Thickness dependence of total shielding efficiency (SE_T) of highly conducting polymers. Sample A: stretched heavily iodine doped Tsukamoto polyacetylene (dotted line is obtained by using approximated α and n), sample B: unstretched heavily iodine doped Tsukamoto polyacetylene, sample C: camphor sulfonic acid doped polyaniline in m-cresol solvent, sample D: PF_6 doped polypyrrole, and sample E: TsO doped polypyrrole. Inset: comparison of σ_{mw} , ε_r, and tan δ. Reprinted with permission from [J. Joo and A. J. Epstein, Appl. Phys. Lett. 65 (18), 2278-2280, 1994]. Copyright [1994], American Institute of Physics.

It can be concluded that SE of PANI and PPY films show weak temperature dependence. However, pronounced thickness effects were observed with attenuation level of -30 to -90 dB depending on thickness and conductivity. Different types of shielding mechanisms i.e. reflection, absorption and multiple reflections were discussed and corresponding theoretical equations were also presented. It has been found that absolute value of tanδ plays a critical role in determining the shielding effectiveness. When tanδ >> 1 (e.g. for heavily doped and highly conducting ICPs or metals), shielding is solely determined by σ. However, when tanδ ~ 1, both σ and ε_r must be considered when calculating absorption coefficient (α) and complex index of refraction (n) which decide overall shielding effectiveness. Therefore, one can expect higher shielding efficiency for materials with higher σ and ε_r.

It has been observed that magnetic properties also play a vital role in improving shielding response. Kathirgamanathan et al (1993) have demonstrated that PPY impregnation microporous membranes such as polyurethane, polyethylene, poly(ethylene terephthalate) (PET), poly(propylene) etc., showed higher SE (~ -10 to -50 dB) in the 10 kHz to 1000 MHz frequency range as compared to metal (e.g. Al) based membranes. The authors pointed out the higher relative magnetic permeability (μ_r>1) due to the incorporation of paramagnetic Fe (III) during the synthesis process provided extra shielding by absorption as compared with the μ_r~1 for aluminum. Furthermore, the microscopic orientation of ICPs is expected to improve SE as showed by the fact that higher SE was exhibited by the PPY impregnated polyethylene membranes (-40 to -45 dB) than that of the impregnated polyurethane membranes (-20 to -25 dB), despite the much lowered thickness (1/5th) which was due to the more oriented PPY produced in polyethylene than that in polyurethane.

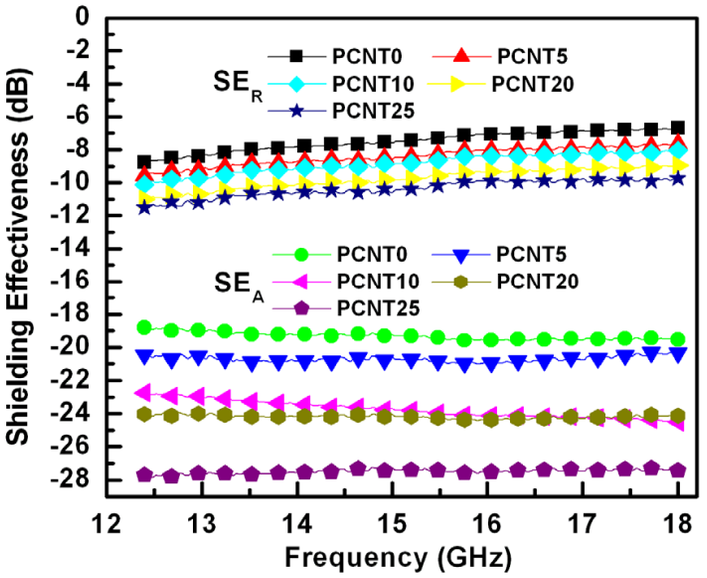

Figure 25. Frequency dependence of losses due to reflection (SE_R) and absorption (SE_A) for MWCNT loaded PANI nanocomposites having different loadings of MWCNT relative to aniline monomer viz. PCNT0 (0.0 wt. %),PCNT5 (5.0 wt. %), PCNT10 (10 wt. %), PCNT20 (20 wt. %) and PCNT25 (25 wt. %).

Synergistic coupling of fillers can give unique combination of properties (Saini et al 2009a) like enhanced conductivity, better dielectric/magnetic traits and improved processability/thermal conductivity that can not be achieved by individual fillers. This ultimately gets resulted in superior shielding performance (Fig. 25) so that reflection loss (SE_R) increases slightly from -8.0 to -12.0 dB whereas absorption loss (SE_A) exhibited rapid enhancement from -18.5 to -28.0 dB with the increase in CNT loading. This may be ascribed to increase in the conductivity (as well as capacitive coupling effects) of composites leading to proportional decrease in skin depth which may be helpful in designing thinner EMI shields. The increased conductivity may manifest itself as increase in both long range charge transport as well as number of possible relaxation modes, leading to enhanced ohmic losses.

The well-dispersed PANI NPs within insulating epoxy matrix provides continuous conducting networks with higher level of charge delocalization which leads to huge

negative permittivity (Hsieh et al, 2012) which is a signature of left handed materials (LHM). The observed EMI SE in an electric field at low frequency (100−1000 MHz) range was found to be -30 to -60 dB.

A straight forward solution for handling low conductivity and poor processability (or agglomeration tendency) of ICPs and CNTs respectively is combining these two fillers in composites. Saini et al (2009a) prepared polyaniline (PANI) coated multiwall carbon nanotubes (MWCNTs) which inherit dielectric and magnetic attributes (ferromagnetism due to entrapped iron phase) from PANI and MWCNT respectively.

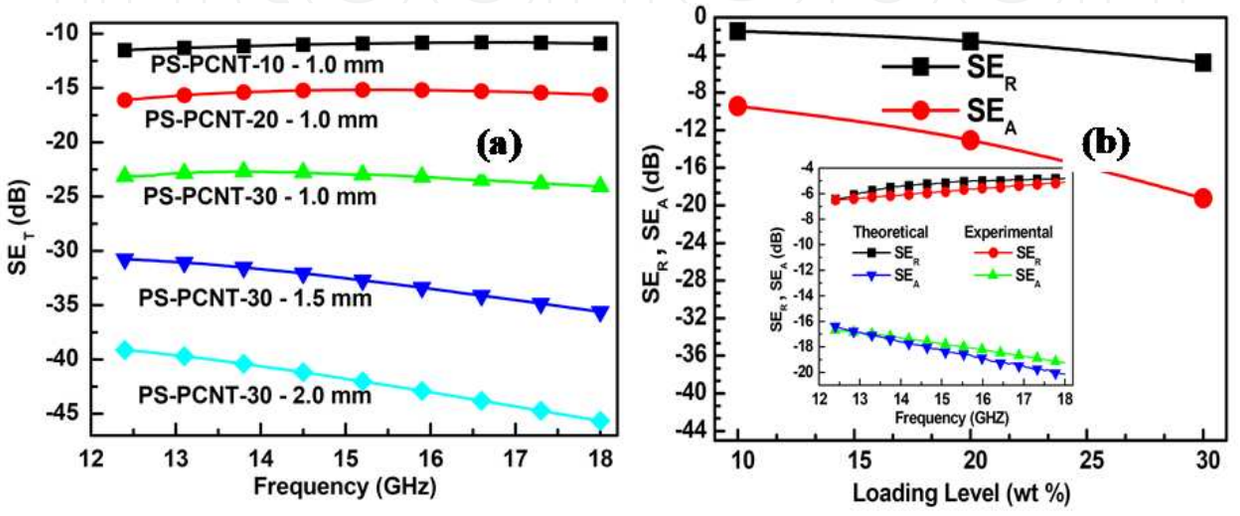

Figure 26. (a) Frequency dependence of SE_T and (b) variation of SE_R and SE_A with loading of PANI-MWCNT. Inset shows the theoretical and experimental SE_R and SE_A value of the composite (PCNT30) in the 12.4 - 18.0 GHz frequency band.

This PANI-MWCNT hybrid filler was solution blended with polystyrene (PS) matrix (10-30 wt % loading) resulting in absorption dominated total shielding effectiveness (SE_T) of -45.7 dB (Fig. 26a) in the 12.4–18.0 GHz range and at a sample thickness of ~2.0 mm. The SE_T was found to exhibit strong dependence on shield thickness as well as loading level of hybrid filler (PANI-MWCNT).

The enhanced SE_T was ascribed to optimization of conductivity, skin-depth, complex permittivity and permeability leading to nominal reflection and high absorption (Fig. 26b). A good agreement between theoretical and experimental shielding measurements (inset of Fig. 26b & Fig. 27) was also observed. Besides, role of highly reflecting planes of PANI-MWCNTs separated with less conducting matrix regions was also explained to introduce multiple reflections resulting in enhancement of absorption loss.

The above studies suggests that ICPs based nanocomposites may give SE value as high as -70 to -80 dB depending on nature of ICP, its loading level and presence of co-fillers. However, high loadings (>30-40%) are required which leads to phase segregation and extreme disturbance of physical properties of host matrices and consequently poor mechanical properties in most cases. Nevertheless, combination of strategies like thin film/membrane technologies, porous structures, negative permittivity materials (or left

handed materials), multilayered structures and hybrid fillers based on broad range of ICP-filler combination are expected to provide an effective solution to realize a lightweight, mechanically strong, processable and economically viable shielding material suitable for commercial and defence sectors.

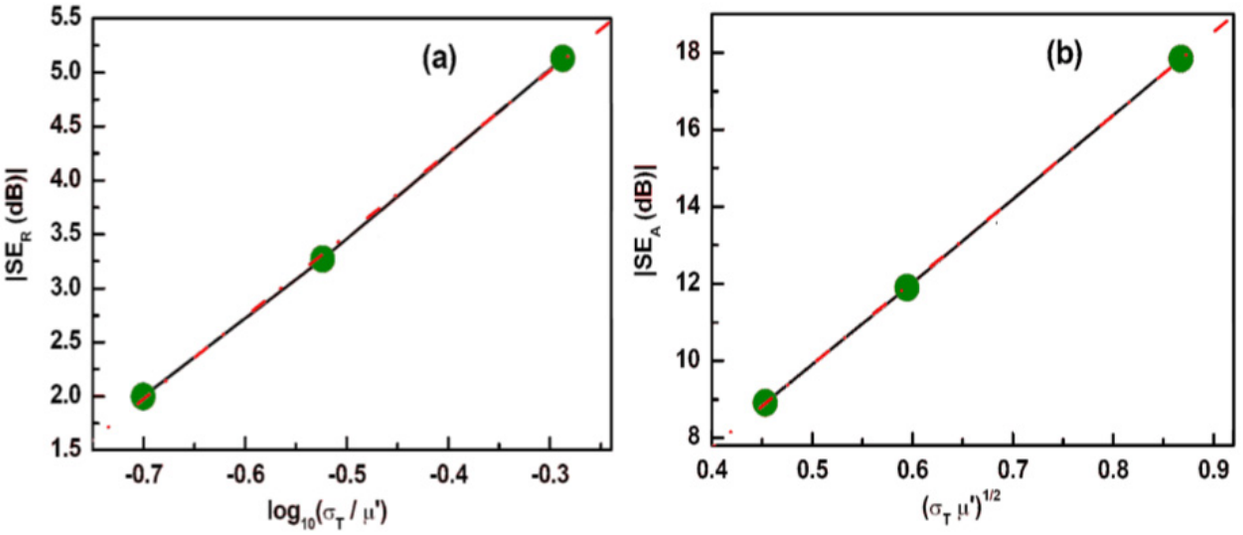

Figure 27. Variation of (a) SER as function of $\log_{10}\left(\frac{\sigma_T}{\mu'}\right)$ and (b) SEA as function of $\left(\sigma_T\mu'\right)^{\frac{1}{2}}$ for PANI-MWCNT filled polystyrene composites

Recently, nanoscale materials based on 2-D graphene sheets have attracted much attention recently due to unusual properties (Geim, 2009; Geim & Novoselov, 2007; Meyer et al, 2007). Like CNTs, here again it is expected that the use of graphene, with large aspect ratio and high conductivity would provide a high EMI SE. Although many studies (In et al, 2010; Liang et al, 2009; Ramanathan et al, 2008; Stankovich et al, 2006; Varrla et al, 2011, Zhang et al, 2011) about the EMI shielding properties of graphene loaded insulating polymer matrix composite systems are available, Basavaraja et al (2011) presented the first EMI shielding results on ICP/oxidized graphene based nanocomposites i.e. Polyaniline/gold-nanoparticles/graphene-oxide (PANI-GNP-GO) based composites in the 2.0-12.0 GHz frequency range. According to authors, the SE values observed for GO and PANI-GNP and PANI-GNP-GO composites were in the ranges -20 to -33 dB, -45 to -69 dB and -90 to -120 dB respectively. However, considering the fact that GO is a poor conductor, conclusion from the presented thickness dependences of above composites and from our own experience, the results seem to be far from realistic. Nevertheless, the graphene nanocomposites research is still at very early stage of evolution especially from the view point of EMI shielding material development.

For many applications e.g. radar absorbers or stealth technology, the sample should reflect as low energy as possible. However, conducting filler loaded composites gives significant reflection (primary shielding mechanism) alongwith absorption which is secondary EMI shielding mechanism. For reduction of reflection loss and significant absorption of the

radiation, the shield should have electric and/or magnetic dipoles which interact with the electromagnetic fields in the incident radiation. Therefore, numerous attempts have also been made to introduce dielectric ($BaTiO_3$, TiO_2 etc.) or magnetic (γ-Fe_2O_3, Fe_3O_4, $BaFe_{12}O_{19}$ etc.) materials within various ICP matrices as filled inclusions (Abbas et al, 2005, 2007; Chan, 1999; Chandrasekhar, 1999; Cho & Kim, 1999; Dong et al, 2008; Ellis, 1986; Gairola et al, 2010; Huang, 1990; Knott et al, 1993; Kurlyandskaya et al, 2007; Meshram et al, 2004; Nalwa, 1997; Ngoma et al, 1990; Pant et al, 2006; Phang et al, 2007, 2008, 2009, 2010; Xiaoling et al, 2006; Xu et al, 2007; Yang et al, 2010, 2011). It has been observed that thickness is an extrinsic parameter that can be adjusted to regulate the shielding offered by a shielding with given permittivity or permeability which can be tuned by nature and concentration of filler. An optimized dielectric particulates filled composite sample based on $BaTiO_3$ and polyaniline in polyurethane matrix (Abbas et al 2005) exhibited a maximum reflection loss of -15 dB (>99% power absorption) at 10 GHz with a bandwidth of 3.0 GHz for a 2.98 mm thick sample. Again the role of thickness and dielectric attributes to modulate absorption was demonstrated by theoretical calculations and experimental results. Similarly, they have also prepared polyaniline-$BaTiO_3$-carbon based composites (Abbas et al 2006) with maximum reflection loss of -25 dB (2.5 mm thick sample) at 11.2 GHz and bandwidth of 2.7 GHz. Many attempts were also made to introduce magnetic losses into the system for example, Yang et al (2009) produced PANI-Fe_3O_4 composites with reflection loss of -2 dB at 14.6 GHz for 3 mm thick sample. Gairola and coworkers (2010) prepared PANI with $Mn_{0.2}Ni_{0.4}Zn_{0.4}Fe_2O_4$ ferrite nanocomposites by mechanical blending with absorption loss of -49.2 dB in the 8.2-12.4 GHz range. Dong et al (2008) synthesized PANI-Ni core shell composites with reflection loss of less than -10 dB in the 4.2–18 GHz range. Phang and coworkers (2009) formulated PANI-HA based nanocomposites containing TiO_2 and Fe_3O_4 nanoparticles as dielectric filler and magnetic filler, respectively. The resultant composites show good microwave absorption response with attenuation of -48.9 dB. Phang et al (2007, 2008) produced PANI nanocomposites containing combination of dielectric (TiO_2) and conducting (CNTs) fillers possessing moderate conductivity and dielectric property with maximum reflection loss of -31 dB (for PANI-TiO_2) at 10 GHz and -21.7 dB (PANI-TiO_2-CNT) at 6GHz. In above composites, use of conducting fillers such as CNTs is expected to improve thermal conductivity (e.g. 0.19 W/mK for PANI and 0.3-0.6 W/mK for PANI-CNT composites) besides extending enhanced shielding performance. Such an improvement in thermal conductivity is beneficial for fast dissipation of heat which is generated due to interaction of shield with high frequency (GHz range) microwave radiations.

4. Conclusions

Although, much work has been done to introduce electrical conductivity in various polymer matrices but high percolation threshold and lower aspect ratios of ICPs compared to metals or carbon based fillers remained a challenging issue. Therefore, considerable work is still needed to improve further the SE as well as mechanical properties of conducting polymer based composites. Synthesis of hybrid filler materials based on various combination of conducting polymers, carbon based materials and dielectric/magnetic nanoparticles seem to be a possible solution. Nevertheless, in the light of current scenario it may be stated that

there is a lot be done to attain a shielding material that can satisfy all the techno commercial specification and maintain the process economics at the same time.

Author details

Parveen Saini and Manju Arora
National Physical Laboratory, New Delhi, India

5. References

Abbas, S.M., Dixit, A.K., Chatterjee, R. and Goel, T.C. 2005, *Mater. Sci. Eng. B*, 123, 167.

Abbas, S.M., Chandra, M., Verma, A., Chatterjee, R. and Goel, T.C. 2006, *Composites: Part A*, 37, 2148.

Abbas, S.M., Chatterjee, R., Dixit, A.K., Kumar, A.V.R. and Goel, T.C. 2007, *J. Appl. Phys.*, 101, 074105.

Ajayan, P.M., Schadler, L.S., Giannaris, C. and Rubio, A. 2000, *Adv. Mater.*, 12, 750.

Ajayan, P.M., Stephan, O., Colliex, C. and Trauth, D. 1994, *Science*, 265, 1212.

Alexandre, M. and Dubois, P. 2000, *Materials Science and Engineering*: *R: Reports*, 28, 1.

Bal, S. and Samal, S.S. 2007, *Bull. Mater. Sci.*, 30, 379.

Baeriswyl, D., Campbell, D.K. and Mazumdar, S. 1992, *Conjugated Conducting Polymers*, Edited by Keiss, H.G. Springer-Verlag, Berlin, 7.

Basavaraja, C.,Kim, W.J., Kim, Y.D. and Huh, D.S. 2011, *Mater. Lett.*, 65, 3120.

Baughman, R.H., Zakhidov, A.A. and Heer, W.A. de 2002, *Science*, 297, 787.

Bredas, J.L., Cornil, K., Meyers, F. and Beljonne, D.1998, *Handbook of Conducting Polymers,* Ed.: Skotheim, T.A., Elsenbaumer, R.L., Reynolds, J.R. and Dekker, M. Inc., New York.

Cao, Y., Smith, P. and Heeger, A.J. 1992, *Synth. Met.*, 48, 91.

Cao, Y., Qiu, J., Smith, P. 1995, *Synth. Met.*, 69, 187.

Carter, G.M., Thakur, M.K., Chen, Y.J. and Hryniewicz, J.V. 1985, *Appl. Phys. Lett*., 47, 457.

Chan, H.L.W., Cheung, M.C. and Choy, C.L. 1999, *Ferroelec.*, 224, 113.

Chandrasekhar, P. 1999, *Conducting Polymers: fundamental and Applications, A Practical Approach*, Kluwer Academic Publishers.

Chandrasekhar, P. and Naishadham, K. 1999, *Synth. Met.*, 105, 115.

Chandrasekhar, P., Zay, B.J., Birur, G.C., Rawal, S., Pierson, E.A., Kauder, L. and Swanson, T. 2002, *Adv. Funct. Mater.*, 12, 2137.

Chiang, C.K., Fincher, C.R.J., Park, Jr., Y.W., Heeger, A.J., Shirakawa, H., Louis, E.J., Gau, S.C. and MacDiarmid, A.G. 1977, *Phys. Rev. Lett.*, 39, 1098.

(a) Chiang, C.K., Gau, S.C., Fincher, C.R.J., Park, Y.W., MacDiarmid, A.G. and Heeger, A.J. 1978, *Appl. Phys. Lett.*, 33, 18.

(b) Chiang, C.K., Druy, M.A., Gau, S.C., Heeger, A.J., Louis, E.J., MacDiarmid, A.G., Park, Y.W. and Shirakawa, H. 1978, *J. Amer. Chem. Soc*., 100, 1013.

Cho, H.S. and Kim, S.S. 1999, *IEEE Trans. Magn.*, 35, 3151.

Choudhary,V. and Gupta, A. 2011, *Carbon Nanotubes-Polymer Nanocomposites*, Ed. Siva Yellampalli, InTech.

Chung, D.D.L. 2000, *J. Mater. Eng. Perform.*, 9, 350.
Chung, D.D.L. 2001, Carbon, 39, 279.
Colaneri, N.F. and Shacklette, L.W. 1992, *IEEE Trans. Instrum. Meas.*, 41, 291.
Coleman, M.M. and Petanck, R.J. 1986, *J. Polym. Sci.*, 16, 821.
Das, C. K. and Mandal, A. 2012, *J. Mater. Sci. Res.*, *1*, 45.
Dhawan S.K., Singh, N. and Rodrigues, D. 2003 *Sci. Technol. Adv. Mater.*, 4,105.
Dong, X.L., Zhang, X.F., Huang, H. and Zuo, F. 2008, *Appl. Phys. Lett.*, 92, 013127.
Ellis, J.R. 1986, *Handbook of Conducting Polymers*, 1st Edition; T.A. Skotheim, Marcel Dekker: New York.
Fang, F.F., Kim, J.H. and Choi, H.J. 2006, *Macromol. Symp.* 2006, *242*, 49.
Freund, M.S. and Deore, B. 2007, *Self-Doped Conducting Polymers*, John Wiley & Sons Ltd., Chichester.
Friend, R.H. 1993, *Rapra Rev. Repo.*, 6
Gairola, S.P., Verma, V., Kumar, L., Dar, M.A., Annapoorni, S. and Kotnala, R.K. 2010, *Synth. Met.*, 160, 2315.
Gangopadhyay, R., De, A. and Ghosh, G. 2001, *Synth. Met.*,123, 21.
Geim, A.K. 2009, *Science*, 324,1530.
Geim, A.K. and Novoselov, K.S. 2007, *Nature Mater*, 6, 183.
Grimes, C.A., 1994, *Aerospace Applications Conference*, 1994. *Proceedings.*, 1994 *IEEE*, 211, Doi: 10.1109/AERO.1994.291194.
Gupta, A. and Choudhary, V. 2011, *Comp. Sci. Technol.*, 71, 1563.
Gupta, S.K., Dhawan, S.K., Arora, M. and Arya S.K. 2005, *Proc. IWPSD*, II, 1318.
(a) Heeger, A.J. 2001, *Angew. Chem. Intern. Ed.*, 40, 2591.
(b) Heeger, A.J. 2001, *Rev. Mod. Phys.*, 73, 681.
Hsieh, C.-H., Lee,A.-H, Liu, C.-D., Han, J.-L., Hsieh, K.-H. and Lee, S.-N. 2012, *AIP Adv.*, 2, 012127.
Hong, Y.K., Lee, C.Y., Jeong, C.K., Lee, D.E, Kim, K., Joo, J., 2003, *Rev. Sci. Instrum.*, 74, 1098.
Huang, Chi-Yuan and Wu, Chang-Cheng 2000, *European Polymer Journal*, 36, 2729.
Huang, Li, N., Du, Y., He, F., Lin, X., Gao, X., Ma, H., Li, Y., Chen, F., Y. and Eklund, P.C. 2006, *Nano letters*, 6, 1141.
Huang, X.X., Chen, Z.F., Zou, W.Q., Liu, Y.S. and Li, J.D. 1990, *Ferroelec.*, 101, 111.
Iijima, S. 1991, *Nature (London)*, 354, 56.
In, K.M., I.K., Lee, J., Ruoff, R.S. and Lee, H. 2010, *Nature Communications*,1, 1067.
Javadi, H.H.S., Cromack, K.R., MacDiarmid, A.G. and Epstein, A.J. 1989, *Phys. Rev. B*, 39, 3579.
Joo, J. and Epstein, A.J. 1994, *Appl. Phys. Lett.*, 65, 2278.
Joo, J., Song, H. G., Jang, K. S., and Oh, E. J. 1999, *Synth. Met.*, 102, 1349.
Joo, J., Oblakowski, Z., Du, G., Pouget, J.P., Oh, E.J., Weisinger, J.M., Min, Y. , MacDiarmid, A.G. and Epstein, A.J. 1994, *Phys. Rev. B*, 49, 2977.
Karasz, F.E., Capistran, J.D., Gagnon, D.R. and Lenz, R.W. 1985, *Mol. Cryst. Liq. Cryst.,* 118, 327.
Kathirgamanathan, P. 1993, Adv. Mater., 5, 281.

Knott, E.F. and Schaeffer, J.F. 1993, *M.T. Radar. Cross Section Handbook*, Artech House: New York.

Koul, S., Chandra, R. and Dhawan S.K. 2000, *Polymer,* 41, 9305.

Kremer F. and Schönhals A. 2003, *Broadband Dielectric Spectroscopy*, Springer Verlag,

Lakshmi, K., John, H., Mathew, K.T., Joseph, R. and George, K.E. 2009, *Acta Materialia*, 57, 371.

Kurlyandskaya, G.V., Cunanan, J., Bhagat, S.M., Aphesteguy, J.C. and Jacobo, S.E. 2007, *J. Phys. Chem. Solids*, 68, 1527.

Liang, J., Wang, Y., Huang, Y., Ma, Y., Liu, Z., Cai, J., Zhang, C., Gao, H. and Chen, Y. 2009, *Carbon*, 47, 922.

MacDiarmid, A.G. 2001, *Angew. Chem. Intern. Ed.*, 40, 2581

Makeiff, D.A. and Huber, T. 2006, *Synth. Met.*, 156, No. 7-8, 497.

Mathur, R.B., Singh, B.P. and Pandey, S. 2010, *Polymer nanotubes nanocomposites, Synthesis properties and applications*, Ed. Vikas Mittal, Wiley Scrivener.

Mattosso, L.H.C., Faria, R.M., Bulhoes, L.O.S., MacDiarmid, A.G. and Epstein, A.J. 1994, *J. Polym. Sci. Part A: Polym. Chem.*, 32, 2147.

Meshram, M.R., Agrawal, N.K., Sinha, B. and Misra, P.S. 2004, *J. Magn. Magn. Mater.*, 271, 207.

Meyer, J.C., Geim, A.K., Katsnelson, M.I., Novoselov, K.S., Booth, T.J. and Roth, S. 2007, *Nature*, 446, 60.

Moniruzzaman, M. and Das, C. K. 2010, *Macromol. Symp.*, *298*, 34.

Moniruzzaman, M. and Winey, K.I. 2006, *Macromolecules*, 39, 5194.

Moon, I.K., Lee, J., Ruoff, R.S. and Lee, H. 2010, *Nature Communications*, 1,1067.

Naishadham, K. and Chandrasekhar, P. 1998, *IEEE Trans. Microw. Theo. Technol.*, 3, 1353.

Naishadham, K. and Kadaba, P.K. 1991, *IEEE Trans. Microw.*, 39, 1158.

Ngoma, J.B., Cavaille, J.Y., Paletto, J., Perez, J. and Macchi, F. 1990, *Ferroelec.*, 109, 205.

Nalwa, H.S. 1997, *Handbook of Organic Conductive Molecules and Polymers* (four volumes), Wiley, New York.

Natta, G., Mazzanti, G. and Corradini, P. 1958 *Atti Accad. Naz Linceicl. Sci. Fis. Mat. Nat. Rend.*, 2, 25.

Nicolson, A.M. and Ross, G. F. 1970, *IEEE Trans. Instrum. Meas.*, 19, 377.

Olmedo L., Hourquebie, P. and Jousse, F. 1997, *Handbook of Organic Conductive Molecules and Polymers*, vol. 2; John Wiley & Sons Ltd, Chichester.

Olmedo, L., Hourquebie, P. and Jousse, F. 1995, *Synth. Met.*, 69, 205.

Ott, H.W. 2009, *Electromagnetic Compatibility Engineering*, New Jersey, John Wiley & Sons.

Pandey, S., Singh, B.P., Mathur, R.B., Dhami, T.L., Saini, P. and Dhawan, S.K. 2009, *Nanoscale Research Letters*, 4, 327.

Pant, H.C., Patra, M.K., Verma, A. , Vadera S.R. and Kumar, N. 2006, *Acta Materialia*, 54, 3163.

Phang, S.W., Hino, T., Abdullah, M.H. and Karamoto, N. 2007, *Mater. Chem. Phys.*, 104, 327.

Phang, S.W., Tadokoro, M., Watanabe, J. and Kuramoto, N. 2008, *Synth. Met*., 158, 251.

Phang, S.W., Tadokoro, M., Watanabe, J. and Kuramoto, N. 2009, *Poly. Adv. Technol.*, 20, 550.

Phang, S.W. and Kuramoto, N. 2010, *Poly. Comp.*, 31, 513.

Pomposo, J.A., Rodriguez, J. and Grande, H. 1999, *Synth. Met*., 104, 107.
Pud, A.,Ogurtsov, N., Korzhenko, A. and Shapoval, G. 2003, *Prog. Poly. Sci*., 28, 1701.
Qiao, R., Yang, C. and Gao, M. 2009, *J. Mater. Chem*., 19, 6274.
Rahman, S., Mahapatra, M., Maiti, M.M. and Maiti, S. 1989, *J. Poly. Mater*., 6, 135.
Ramanathan T, Abdala, A.A., Stankovich, S., Dikin, D.A., Herrera-Alonso, M., Piner, R.D., Adamson, D.H., Schniepp, H.C., Chen, X., Ruoff, R.S., Nguyen, S.T., Aksay, I.A., Prud'Homme, R.K. and Brinson L.C. 2008, *Nature Nanotechnol*, 3, 31.
Ramasubramaniam, R., Chen, J. and Liu, H. 2003, *Appl. Phys. Lett*., 83, 2928.
Riande, E. and Diaz-Calleja, R. 2004, *Electrical Properties of Polymers*, CRC Press ISBN: 978-1-4200-3047-1.
Rozenberga, B.A., and Tenn, R. 2008, *Prog. Polym. Sci*., 33, 40.
Saini, P., Choudhary, V. and Dhawan, S. K., 2007, *Ind. J. Engn. Mater. Sci*., 14, 436.
Saini, P., Choudhary, V. and Dhawan, S.K. 2010, *Poly. Adv. Technol*., 21, 1.
Saini, P., Jalan, R. and Dhawan, S.K. 2008, *J. Appl. Polym. Sci*., 108, 1437.
(a) Saini, P., Choudhary, V., Singh, B.P., Mathur, R.B. and Dhawan, S.K. 2009, *Mater. Chem. Phys*., 113, 919,
(b) Saini, P., Choudhary, V., Sood, K.N. and Dhawan, S.K. 2009, *J. Appl. Poly. Sci*., 113, 3146.
Saini, P., Choudhary, V., Singh, B.P., Mathur, R.B. and Dhawan, S.K. 2011, *Synth. Met*., 161, 1522.
Sanjai, B., Raghunathan, A., Natarajan, T.S., Rangarajan, G., Thomas, S. Prabhakaran, P.V. and Venkatachalam, S. 1997, *Phys. Rev. B*, 55, 10734.
Savitha, P., Rao, P.S. and Sathyanarayana, D.N. 2005, *Polym. Int*., 54, 1243.
Saxman, A.M., Liepins, R. and Aldissi, M. 1985, *Prog. Polym. Sci*., 11, 57.
Schelkunoff, S.A. 1943, *Electromagnetic Waves*, Van Nostrand, New Jersey.
Sheng, P. and Klafter, J. 1983, *Phys. Rev. B*., 27, 2583.
Schulz, R.B., Plantz, V.C. and Brush, D.R. 1988, *IEEE Trans*., 30, 187.
Shacklette, L.W., Colaneri, N.F., Kulkarni, V.G. and Wessling, B. 1992, *J. Vinyl Technol*., 14, 118.
Shi, Sui-Lin and Liang, Ji, 2008 *Nanotechnology,* 19, 255707.
Shirakawa, H. 2001, *Angew. Chem. Intern. Ed*., 40, 2575.
Shirakawa, H., Louis, E.J., MacDiarmid, A.G., Chiang, C.K. and Heeger, A.J. 1977, *Chem. Comm*., 578.
Skotheim, T.A. 1986, *Handbook of Conducting Polymers*, 2nd Edition, CRC.
Sillars, R.W. 1937, J. Inst. Elect. Eng., 80, 378
Singh, B.P., Prabha, Saini, P., Gupta, T., Garg, P., Kumar, G., Pandey, I., Pandey, S., Seth, R.K., Dhawan, S.K. and Mathur, R.B. 2011, *J. Nanopart. Res*., 1.
Singh, P., Babbar, V.K., Razdan, A., Srivastava, S.L. and Goel, T.C. 2000, *Mater. Sci. Eng. B*, 78, 70.
Singh, P., Babbar, V.K., Razdan, A., Srivastava, S.L. and Puri, R.K. 1999, *Mater. Sci. Eng. B*, 67, 132.
Snow, A.W. 1981, *Nature*, 292, 40.
Soga, K., Nakamura, M., Kobayashi, Y. and Ikeda, S. 1983, *Synth.. Met*., 6, 275.

Stafstrom, S., Bredas, J.L., Epstein, A.J., Woo, H.S., Tanner, D.B., Huang, W.S. and MacDiarmid, A.G. 1987, *Phys. Rev. Lett.*, 59, 1464.

Stankovich, S., Dmitriy, A.D., Geoffrey, H.B.D., Kevin, M.K., Zimney, E.J., Stach, E.A., Piner, R.D., Nguyen, S.T. and Ruoff, R.S. 2006, *Nature*, 442, 20.

Stankovich, S., Dikin, D.A., Piner, R.D., Kohlhaas, K.M., Kleinhammes, A, Jia, Y., Wu, Y., SonBinh, T. N., Rodney, S.R. 2007, *Carbon*, 45, 1558.

Stonier, R.A. 1991, *Sampe J.*, 27, 9.

Taka, T. 1991, *Synth. Met.*, 41, 1177.

Thomas, B., Pillai, M.G.K. and Jayalakshmi, S. 1988, *J. Phys. D: Appl. Phys.*, 21, 503.

Thostenson, E.T., Li, C. and Chou, T.-W. 2005, *Nanocomposites in context, Composites Science and Technology*, 65, 491.

Tong, X.C., 2009, *Advanced Mater. And Design For Electromagnetic Interference Shielding*, CRC Press Taylor and Francis Book, London, New York.

Trivedi, D.C. 1997, *Handbook of Organic Conductive Molecules and Polymers*, 2, John Wiley & Sons Ltd.: Chichester

Varrla, E., Venkataraman, S. and Sundara R. 2011, *Macromol. Mater. Eng.*, 296, 894.

Wang, Y. and Jing, X., 2005, *Polym. Adv. Technol.*,16, 344.

Wang, Z.H., Li, C., Scherr, E.M., MacDiarmid, A.G. and Epstein, A.J. 1991, *Phys. Rev. Lett.*, 66, 1745.

Wagner, K.W . 1914, *Arch Elektrotech*, 2, 371.

Weir, W.B. 1974, *Proc. IEEE*, 62, 33.

Wessling, B. 1999, *Synth. Met.*, 102, 1396.

Wojkiewicz, J.L., Fauveaux, S. and Miane, J.L. 2003, *Synth. Met.*,135–136, 127

Xiaoling, Y., Gang, L., Duanming, Z. and Huahui, H. 2006, *Mater. Design*, 27, 700.

Xu, P., Han, X.J., Jiang, J.J., Wang, X.H., Li, X.D. and Wen, A.H. 2007, *J. Phys. Chem. C*, 111, 12603.

Yamamoto, T., Hayashi, Y. and Yamamoto, A. 1978, *Bull. Chem. Soc. Japan*, 51, 2091.

Yang, C., Du, J., Peng, Q., Qiao, R., Chen, W., Xu, C., Shuai, Z. and Gao, M. 2009, *J. Phys. Chem. B*, 113, 5052.

Yang, C.C., Gung, Y.J., Hung, W.C., Ting, T.H. and Wub, K.H. 2010, *Composites Science and Technology*, 70, 466.

Yang, C.C., Gung, Y.J., Shih, C.C., Hung, W.C. and Wub, K.H. 2011, *J. Magn. Magn. Mater.*, 323, 933.

(a) Yang, Y., Gupta, M.C., Dudley, K.L. and Lawrence, R.W. 2005, *Nano Lett.*, 5, 2131.

(b) Yang, Y., Gupta, M.C., Dudley, K.L. and Lawrence, R.W. 2005, *Adv. Mater.*, 17, 1999.

Zhang, H.-B., Yan, Q., Zheng, W.-G., He, Z. and Yu, Z.-Z.T. 2011, *ACS Appl. Mater. Interfaces*, 3, 918.

Zuo, F., Angelopoulos, M., MacDiarmid, A.G. and Epstein, A.J. 1989, *Phys. Rev. B*, 39, 3570.